of performing toxicology tests and FDA approvals for each individual antisense sequence; a formidable barrier to clinical application. Skipping of more than one exon could, theoretically, increase the applicability to some 90% of DMD patients[7,8] while aiming to produce the most functionally favorable dystrophin variants.[7]

The canine X-linked muscular dystrophy (CXMD) harbors a point mutation within the acceptor splice site of exon 7, leading to exclusion of exon 7 from the mRNA transcript.[9] We used the Beagle model here, the mutation of which originates from the Golden Retriever model, but which is less severely affected. At least two further exons (exons 6 and 8; Fig 1) must be skipped (multiexon skipping) to restore the open reading frame; therefore, it is more challenging to rescue dystrophic dogs with an exon-skipping strategy. Previously, McClorey and colleagues[10] showed transfection with antisense oligo targeting exons 6 and 8 restored reading frame of mRNA in cultured myotubes from dystrophic dogs *in vitro*. Here, we identified a phosphorodiamidate morpholino oligomer (PMO) cocktail that, using either intramuscular injection or systemic intravenous delivery, was not toxic, resulted in extensive dystrophin expression to therapeutic levels, and was associated with significant functional stabilization in dystrophic dogs *in vivo*.

Methods

Animals

CXMD-affected dogs and wild-type littermates from 2 months to 5 years old were used in this study[11] (see the Supplementary Table). Institutional animal care and use committee of National Center of Neurology and Psychiatry Japan approved all experiments using CXMD.

Antisense Sequences and Chemistries

We designed four antisense sequences to target exons 6 and 8 of the dog dystrophin mRNA as follows: Ex6A (GTTGATTGTCGGACCCAGCTCAGG), Ex6B (ACCTATGACTGTGGATGAGAGCGTT), Ex8A (CTTCCTGGATGGCTTCAATGCTCAC), and Ex8B (ACCTGTTGAGAATAGTGCATTTGAT). Sequences were designed to target exonic sites of exon 6 (Ex6A) and exon 8 (Ex8A), or exon/intron boundary between exon 6 and intron 6 (Ex6B), or exon 8 and intron 8 (Ex8B) (see Fig 1). Two donor-site sequences (Ex6B and Ex8B) were designed to target 23bp of exon and 2bp of intron. Sequences were synthesized using two different backbone chemistries: 2′O-MePs (Eurogentec Liège, Belgium), and morpholino (Gene-Tools, LLC Philomath, OR).[12] We determined these sites based on the exonic splicing enhancer motifs, GC contents, and secondary structures. We also avoided self/heterodimers. U (uracil) was used instead of T (thymidine) for the synthesis of 2′O-MePs oligos. A discussion and fig-

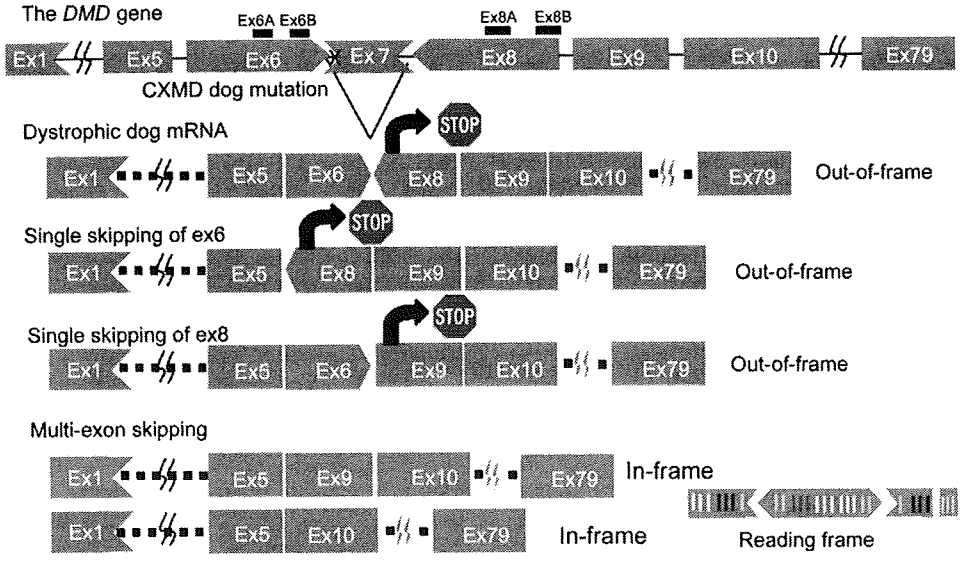

Fig 1. Mutation in canine X-linked muscular dystrophy (CXMD) and strategy for exon-skipping treatment. The dystrophic dog harbors a point mutation at splice site in intron 6, which leads to lack of exon 7 in messenger RNA. Single-exon skipping of exon 6 or 8 leads to out-of-frame products. Exclusion of at least two further exons (exons 6 and 8) is required to restore reading frame. Each extremity of the box represents the specific phasing of the exon. Left end of exons: 1: vertical lane (such as exon 6) means that the exon begins by the first nucleotide of a codon; 2) arrowhead toward left (such as exon 8) means that the exon begins by the second nucleotide of a codon; and 3) arrowhead toward right (such as exon 7) means that the exon begins by the third nucleotide of a codon. Right end of exons: 1) Vertical lane (such as exon 8) means that the exon ends by the last nucleotide of a codon; 2) arrowhead toward left (such as exon 1) means that the exon ends by the first nucleotide of a codon; and 3) arrowhead toward right (such as exon 6) means that the exon ends by the second nucleotide of a codon. DMD = Duchenne muscular dystrophy.

ure showing the alternative chemistries can be found in Yokota and colleagues' article.[13]

In Vitro Cell Transfections

Primary myoblast cells from neonatal CXMD dogs were obtained by standard methods using a preplating method.[14] Normal control (wild-type) or dystrophic (CXMD) myoblasts (1.5×10^5 cells) were cultured in growth medium containing F-10 growth media, 20% fetal calf serum, basic fibroblast growth factor (2.5ng/ml), penicillin (200U/ml), and streptomycin (200μg/ml) for 72 hours, followed by antisense oligonucleotide (2'O-MePs) administration (0.25–5μg/ml, 30–600nM) for 3 hours with lipofectin (Invitrogen, La Jolla, CA) following manufacturer's instructions (Antisense Oligo (AO)/lipofectin ratio = 1:2). The cells were cultured in differentiation medium containing Dulbecco's minimum essential medium with Horse Serum (HS) (2%), penicillin (200U/ml), and streptomycin (200μg/ml) for 4 to 5 days before analyses for RNA and protein. Morpholino antisense oligonucleotides carry no charge and cannot be transfected into cells efficiently, so only 2'O-MePs chemistry was utilized for *in vitro* studies.

Intramuscular Injections

Animals were anesthetized with thiopental sodium induction and maintained by isoflurane for all intramuscular injections and muscle biopsies. Skin was excised over the site of injection, muscle exposed, and the injection site marked with a suture in the muscle. Antisense oligonucleotides were delivered by intramuscular injection using 1ml saline bolus into the tibialis anterior or extensor carpi ulnaris (ECU) muscles using a 27-gauge needle. Antisense oligonucleotides were delivered either singly or in mixtures. Both 2'O-MePs and morpholino chemistries were tested. Muscle biopsies were obtained at 2 weeks after antisense injection.

Intravenous Systemic Delivery

Three dogs were treated and all were given an equimolar mixture of morpholinos Ex6A, Ex6B, and Ex8A at 32mg/ml each. Between 26 and 62ml was injected into the right saphenous vein using a 22-gauge indwelling catheter, leading to a cumulative (combined) dose of 120 to 200mg/kg per injection. Morpholinos were injected 5 to 11 times at weekly or biweekly intervals (see the Supplementary Table). Tissues were examined 2 weeks after the last injection.

Reverse Transcriptase Polymerase Chain Reaction and Complementary DNA Sequencing

Total RNA was extracted from myoblasts or frozen tissue sections using TRIzol (Invitrogen). Then reverse transcriptase polymerase chain reaction (RT-PCR) was performed on 200ng of total RNA for 35 cycles of amplification using One-Step RT-PCR kit (Qiagen, Chatsworth, CA) following manufacturer's instructions with 0.6mM of either an exon 5 (CTGACTCTTGGTTTGATTTGGA) or an exon 3/4 junction (GGCAAAAACTGCCAAAAGAA) forward primer. Reverse primers were either exon 10 (TGCTTCGGTCTCTGTCAATG) or exon 13 (TTCATCGACTACCACCACCA). The resulting PCR bands were extracted by using Gel extraction kit (Qiagen). BigDye Terminator v3.1 Cycle Sequencing Kit (Applied Biosystems) was used for complementary DNA sequencing with the same primers.

Hematoxylin and Eosin and Immunostaining

Eight micrometer cryosections were cut from flash-frozen muscle biopsies at an interval of every 200μm, then placed on poly-L-lysine–coated slides and air-dried. Anti-dystrophin rod (DYS-1) or C-terminal monoclonal Ab (DYS-2) (Novocastra Newcastle upon Tyne, UK) were used as primary antibodies. Rabbit anti-neuronal nitric oxide synthase (anti-nNOS) (Zymed Laboratory, San Francisco, CA) was used for nNOS staining. Alexa 468 or 594 (Invitrogen) was used as secondary antibody. 4',6-diamidino-2-phenylindole containing mounting agent (Invitrogen) was used for nuclear counterstaining (blue). The number of positive fibers for DYS-1 was counted and compared in sections where their biggest number of the positive fibers was as described previously.[15] Hematoxylin and eosin staining was performed with Harris hematoxylin and eosin solutions. Images were analyzed and quantified by using ImageJ software.[16]

Western Blotting Analysis

Muscle proteins from cryosections were extracted with lysis buffer containing 75mM Tris-HCl (pH 6.8), 10% sodium dodecyl sulfate, 10mM EDTA, and 5% 2-mercaptoethanol. Four to 40μg proteins were loaded onto precase 5% resolving sodium dodecyl sulfate polyacrylamide gel electrophoresis gels following manufacturer's instructions. The gels were transferred by semidry blotting (Bio-Rad Hercules, CA) at 240mA for 2 hours. DYS-2 (Novocastra) antibody against dystrophin, rabbit polyclonal antibody against α-sarcoglycan, and rabbit polyclonal antibody desmin were used as primary antibodies.[17] Horseradish peroxidase–conjugated anti–mouse or anti–rabbit goat immunoglobulin (Cedarlane Laboratories, Hornby, Ontario, Canada) was used as secondary antibodies. Enzyme chemiluminescence kit (GE Fairfield, CT) was used for the detection. Blots were analyzed by ImageJ software.

Blood Tests

Creatine kinase activity, blood counts, serum biochemistry, and toxicology test in canine serum were assayed with the Fuji Drychem system (Fuji Film Medical Co. Ltd, Tokyo, Japan) and Sysmex F-820 (Sysmex Corporation, Kobe, Japan) according to manufacturer's instruction.

Magnetic Resonance Imaging

For imaging studies, animals were anesthetized with thiopental sodium and maintained by isoflurane. We used a superconducting 3.0-Tesla magnetic resonance imaging (MRI) device (MAGNETOM Trio; Siemens Solutions, Erlanger, Germany) with an 18cm diameter/18cm length human extremity coil. The acquisition parameters for T2-weighted imaging were TR/TE = 4,000/85 milliseconds, slice thickness = 6mm, slice gap = 0mm, field of view = 18 × 18cm, matrix size = 256 × 256, and number of acquisitions = 3 during fast spin echo.

Functional Testing

Clinical evaluation of dogs was performed as described in our previous report.[18] Grading of clinical signs in CXMD dogs was as follows: gait disturbance: grade 1 = none, grade 2 = sitting with hind legs extended, grade 3 = bunny hops with hind legs, grade 4 = shuffling walk, and grade 5 = unable to walk; mobility disturbance: grade 1 = none, grade 2 = lying down more than normal, grade 3 = cannot jump on hind legs; grade 4 = increasing difficulty moving around, and grade 5 = unable to get up and move around; limb or temporal muscle atrophy: grade 1 = none, grade 2 = suspect hardness, grade 3 = can feel hardness or apparently thin, grade 4 = between grades 3 and 5, and grade 5 = extremely thin or hard; drooling: grade 1 = none, grade 2 = occasionally dribbles saliva when sitting, grade 3 = some drool when eating and drinking, grade 4 = strings of drool when eating or drinking, and grade 5 = continuous drool; macroglossia: grade 1 = none, grade 2 = slightly enlarged, grade 3 = extended outside dentition, grade 4 = enlarged and slightly thickened, and grade 5 = enlarged and thickened; dysphagia: grade 1 = none; grade 2 = takes time and effort in taking food, grade 3 = difficulty in taking food from plate, grade 4 = difficulty in chewing, swallowing, or drinking, and grade 5 = unable to eat.

For timed running tests, each dog was encouraged to run down a hallway (15m), and elapsed time was recorded. Single tests were done because dystrophic dogs tired rapidly.

Results

In Vitro Screening of Antisense Oligonucleotides in Dog Primary Myoblasts

The CXMD dog harbors a splice-site mutation of exon 7, leading to an out-of-frame mRNA transcript fusing exons 6 to 8 (see Fig 1). Both exons 6 and 8 must be excluded (skipped) from the mRNA to restore the reading frame. Four antisense oligonucleotides were designed against exons 6 and 8. Ex6A and Ex8A were designed to bind exonic splicing enhancers, and Ex6B and Ex8B were directed against the 5′ splice boundaries of each exon (see Fig 1). The four AOs were transfected as 2′O-MePs either singly or in mixture (cocktails; 5μg/ml each or 600nM each) into cultures of primary myoblasts isolated from the skeletal muscle of neonatal CXMD dogs. Four days after differentiation into myotubes, RNA was isolated and tested for specific exon skipping by RT-PCR. A cocktail of all 4 AOs produced a single 101bp band with 100% of RT-PCR product corresponding to a desired in-frame splice product of exons 5 to 10 (Fig 2A). It is of interest that exon 9, known to be an alternatively spliced exon in the dystrophin mRNA, was consistently skipped, although no antisense oligonucleotide was used against this exon (see Fig 2; see Supplemental Fig 1).[10] Each of the four sequences was also transfected individually, and either Ex6A or Ex6B successfully induced skipping as a single AO (100% in-frame product) (see Fig 2A). The precise skipping of exons was confirmed by complementary DNA sequencing (see

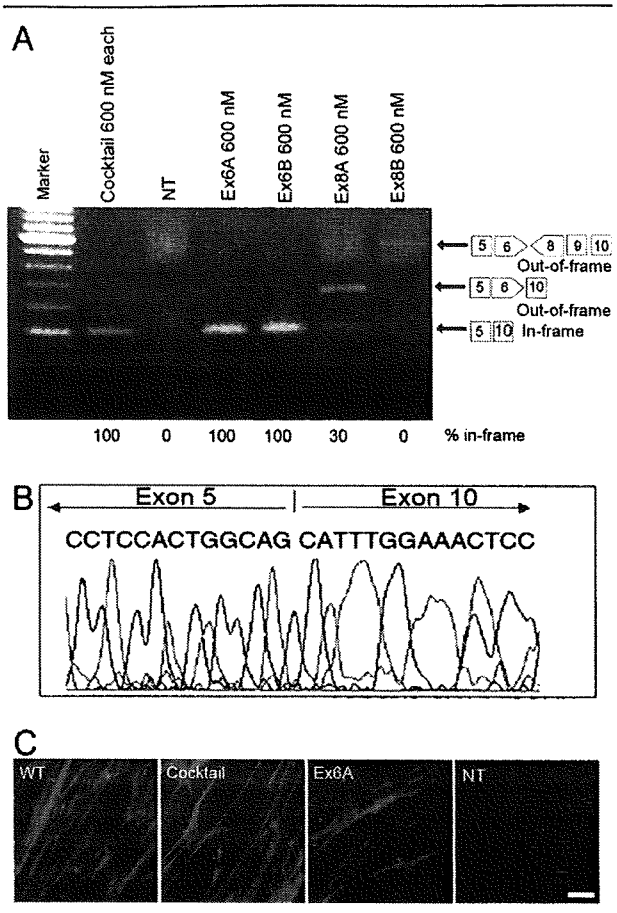

Fig 2. In vitro screening of antisense oligonucleotides and recovery of dystrophin expression by single antisense oligos in dog primary myoblasts. (A) Detection of exons 6 to 9 skipped in-frame products (101bp) using reverse transcriptase polymerase chain reaction (RT-PCR) at 4 days after the transduction of 5μg (600nM) each AOs of single (Ex6A or Ex6B) or cocktail AOs (Ex6A, Ex6B, Ex8A, and Ex8B) as indicated. A faint 585bp out-of-frame band is detected in Ex8B-treated myotubes. Nontreated myotubes (NT) show little RT-PCR product, likely because of nonsense-mediated decay. (B) Complementary DNA (cDNA) sequencing after antisense oligonucleotide treatment at 4 days after the transduction of Ex6A alone, showing the desired in-frame exons 5 to 10 skip. (C) Immunocytochemistry with dystrophin C-terminal antibody (Dys-2; red) and nuclear counterstaining (blue) for primary myotubes from canine X-linked muscular dystrophy (CXMD) cells at 4 days after transfection with cocktail or single antisense 2′O-methylated phosphorothioate (2′O-MePs) targeting exons 6 and 8 (5μg each/ml, or 600nM), non-treated wild-type (WT) cells, and CXMD cells. Scale bar = 50μm.

Fig 2B). We found a dose–response relation where use of 30 and 60nM of either Ex6A or Ex6B induced multiexon skipping of exons 5 to 10, although with less efficiency and more intermediate out-of-frame products (see Supplemental Fig 1A). In contrast, the Ex8A AO alone induced skipping of mainly exons 8 and 9, an

out-of-frame transcript, whereas the Ex8B AO induced no detectable exon skipping (see Fig 2A). Dystrophin protein production from in-frame mRNA was confirmed by immunocytochemistry using either the four-sequence cocktail or Ex6A alone (see Fig 2C).

We tested the same sequences in normal (wild-type) control Beagle cells (see Supplemental Fig 1B-C). When transfected into wild-type Beagle myoblasts, exon 9 was again routinely removed from the transcripts. The antiexon 8 AO pair excised exon 8, similar to dystrophic cells, whereas the exon 6–specific AO pair excised exon 6, as well as exon 9, but left exons 7 and 8 in place.

Efficient Skipping In Vivo Requires a Three-AO Cocktail

Given that Ex8B appeared ineffective by all *in vitro* assays, we did not continue with this sequence. Intramuscular injections were done using Ex6A alone, and equimolar mixtures of Ex6A, Ex6B, and Ex8A. Intramuscular injections into the tibialis anterior or ECU muscles of 0.5- to 5-year-old CXMD dogs were done for both 2'O-MePs and morpholino chemistries, at a dose of 0.12 to 1.2mg of each sequence (Fig 3; see Supplemental Fig 2). Biopsies were performed 2 weeks later at injection sites, marked by suture threads. Dystrophin-positive fibers were concentrated around the injection site, and the absolute number of dystrophin-positive fibers was counted in cross section.

In contrast with the skipping patterns observed with *in vitro* cell transfections, injection of Ex6A alone induced skipping of only exon 6 in experiments using either morpholinos or 2'O-MePs chemistries (see Fig 3; see Supplemental Fig 2). By contrast, the cocktail of Ex6A, Ex6B, and Ex8A induced robust dystrophin expression in a highly dose-dependent manner), with 1.2mg per each morpholino showing areas of complete dystrophin rescue, and high levels of dystrophin by immunohistochemical analysis and immunoblot (see Figs 3A, B, D; see Supplemental Fig 2). Intramuscular injections using the same cocktail with 2'O-MePs chemistry showed similar results, with greater dystrophin rescue using the three AO cocktail compared with Ex6A alone (see Fig 3C). Two pairwise combinations of Ex8A with either Ex6A or Ex6B were tested with morpholino chemistry, and neither combination proved as efficient as the three-sequence cocktail (see Fig 3B).

RT-PCR analyses of injected muscles showed that the Ex6A/Ex6B/Ex8A morpholino cocktail drives efficient skipping of exons 6 to 10 skipped products, with between 61 and 83% of RT-PCR products showing the desired in-frame product in the three muscles tested (see Fig 3D). Additional out-of-frame products were observed with Ex6A alone, and as a minority of products in the cocktail-treated muscles (see Fig 3D).

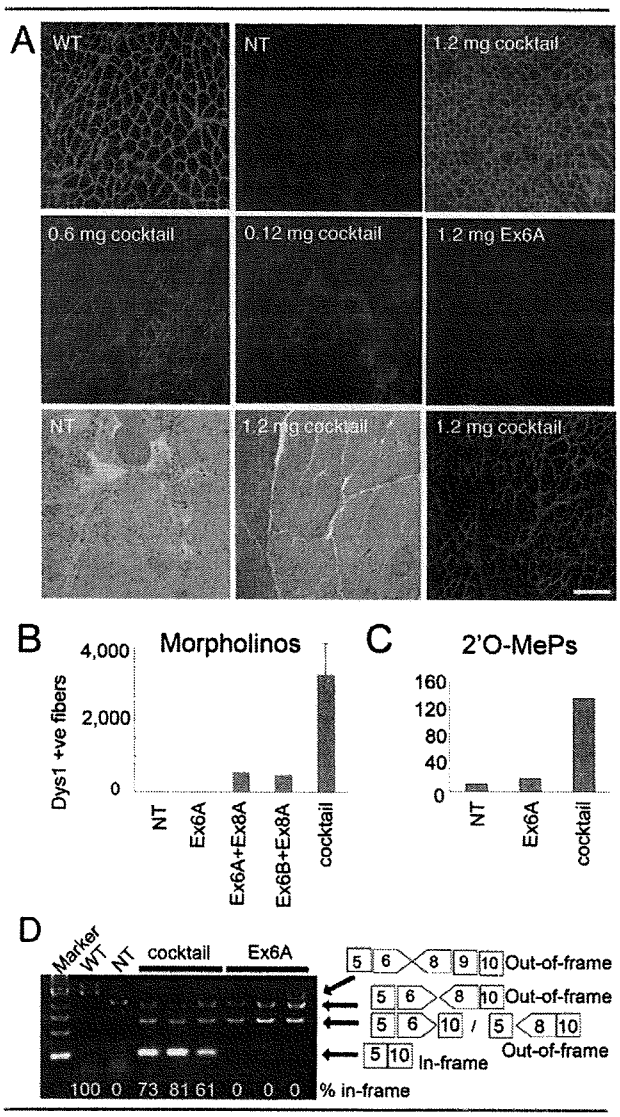

Fig 3. Recovery of dystrophin expression by in vivo intramuscular injection of a three-AO cocktail but not Ex6A alone. (A) Restoration of dystrophin expression in tibialis anterior (TA) at 14 days after single injection with 1.2mg Ex6A only, or cocktail containing 0.12mg each, 0.6mg each, or 1.2mg each of antisense morpholino Ex6A, Ex6B, and Ex8A are shown. Age-matched nontreated (NT) canine X-linked muscular dystrophy (CXMD) and wild-type (WT) dogs are shown as control animals. Hematoxylin and eosin (HE) staining at 14 days after 1.2mg each of the cocktail injection and age-matched nontreated control (NT), with consecutive cryosection stained with dystrophin (DYS-1) and 4',6-diamidino-2-phenylindole, show histological correction of the dystrophy. Bar = 100μm. (B, C) The number of DYS-1–positive fibers in TA or extensor carpi ulnaris (ECU) at 14 days after a single injection with cocktail (Ex6A+Ex6B+Ex8A), or indicated combinations, at 1.2mg each (morpholino; B), or 120μg each 2'O-methylated phosphorothioate (2'O-MePs) (C). Values are mean ± standard error of the mean. (D) RT-PCR analysis at 2 weeks after intramuscular injection of cocktail or Ex6A morpholino at 1.2mg each. The percentage of the in-frame exon 5 to 10 skip is shown under the gel image for treated muscle; normal control (WT) muscle shows the normal full-length in-frame transcript at the expected 100%.

Histological analyses of the muscle injected with the three-morpholino cocktail (1.2mg/each) showed significant histological improvement of the dystrophy, relative to uninjected muscle, (see Fig 3A; bottom panels).

By immunoblotting, intramuscular injection of the optimal cocktail induced dystrophin to 50% normal levels in a 2-year-old dog but only to 25% in a more clinically severe 5-year-old dog (see Supplemental Fig 2A). This result implies that the muscle quality influences the amount of dystrophin that can be produced.

Intravenous Systemic Delivery of a Morpholino Cocktail Induces Body-Wide Dystrophin Expression

AOs must be deliverable systemically to be of therapeutic value. Accordingly, we undertook intravenous infusion of the three morpholino-cocktail showing the most success in the intramuscular experiments (Ex6A, Ex6B, and Ex8A). Three CXMD dogs were studied using intravenous doses similar to that used in *mdx* mouse studies (30–40mg/kg per injection), with weekly or biweekly dosing. The first dog received 120mg/kg morpholinos (40mg/kg per each sequence) in weekly intravenous injections, with five doses over 5 weeks. The second dog was given the same dose 11 times at 2-week intervals over the course of 5.5 months. The third dog received a greater dose: 200mg/kg (66mg/kg of each morpholino) seven times at weekly intervals (see the Supplementary Table). All dogs were euthanized 2 weeks after the last injection, and multiple muscles were examined.

All skeletal muscles of each treated dog showed evidence of *de novo* dystrophin expression by immunofluorescence of cryosections, although the degree of rescue was variable (Fig 4A). Histopathology was markedly improved in regions showing high dystrophin expression (see Fig 4A). Immunoblotting confirmed expression up to approximately 50% of normal levels, but some muscles expressed only trace amounts (see Figs 4C, D). Dystrophin expression was also detected in cardiac muscles but, as in the *mdx* mouse,[19] less than in skeletal muscles and concentrated in small patches (see Fig 4A). Of the three dogs, the average dystrophin protein expression level was greatest in the dog given seven weekly doses of 200mg/kg PMO, with an average of 26% of normal dystrophin levels.

Selected muscles were studied for quantitative rescue of histopathology and for biochemical rescue of dystrophin-interacting proteins (dystrophin-associated glycoproteins and nNOS). A commonly utilized quantitative marker for muscle pathology is central nucleation of myofibers, where increased central nucleation is reflective of increased degeneration and regeneration. Quantitation of central nucleation in treated dogs compared with untreated littermates showed that intravenous antisense treatment reduced central nucleation in all five muscle groups examined (see Fig 4B).

Both nNOS and α-sarcoglycan are dystrophin-associated proteins that colocalize with dystrophin in normal muscle and are reduced in DMD muscle. nNOS immunofluorescence and α-sarcoglycan immunoblotting were done on a series of muscles from treated and control dogs. By immunoblot, α-sarcoglycan was seen to be increased in all muscles examined (Fig 5B). Likewise, nNOS was seen to relocalize to the membrane in dystrophin-positive regions in systemically treated dogs (see Fig 5A).

Muscle Imaging and Clinical Grading Scores Are Improved by Systemic Antisense Treatment

A global improvement in muscle pathology was further supported by the T2-weighted MRI examination (Fig 6). The high-intensity T2 signal, indicative of inflammation and increased water content, was diminished in PMO-treated dogs compared with pretreated and untreated control dogs in most muscles (see Fig 6).

Functional improvement of treated dogs was also assessed by a 15m timed running test and by a combined clinical grading score, as we have previously published.[18] Three dogs treated with intravenous morpholinos were compared with three untreated, at the ages of both 2 or 5 months (pretreatment) and 4 or 7 months (posttreatment) (Figs 7B, C). The untreated littermates became slower over the treatment time, whereas all treated dogs ran faster after treatment. The single dog treated at an older age with more advanced symptoms showed greater improvement relative to untreated littermates (see Fig 7B).

The combined clinical grading score similarly showed improvement or stabilization of disease progression after antisense treatment, relative to natural history controls (see Fig 7A). Videos documenting running ability of treated dogs and untreated littermates are available as supplemental data (see Supplemental Movies 1–5).

Serum creatine kinase was assessed before and after intravenous treatment, and compared with natural history controls (see Supplemental Fig 3). Although serum creatine kinase was variable, posttreatment creatine kinase levels were consistently less than natural history controls.

Intravenous High-Dose Morpholino Cocktail Shows No Evidence of Toxicity

No local inflammatory reactions or organ dysfunctions were recorded in the morpholino-treated dogs. Twice-weekly serum toxicology screens of the three systemically treated dogs showed no evidence of liver or kidney dysfunction (see Supplemental Fig 4). Levels of urea nitrogen, α-glutamyl transpeptidase, and creatinine all remained within the reference ranges. In addition, no significant changes were observed in amylase, total protein, total bilirubin, C-reactive protein, sodium, potas-

sium, or chloride. Growth of body weight was also within reference range in all treated dogs (data not shown).

Discussion

This is the first report of widespread induction of dystrophin expression to therapeutic levels in the dog model of DMD. Overall, our findings provide a promising message for DMD patients. Specifically, we show that intravenous morpholino antisense (PMOs) can generate body-wide production of functional dystrophin in a model clinically more severe than DMD, resulting in stabilization or improvement of the clinical disease. Beneficial effects were documented by histology, MRI, and functional tests (running and combined clinical grading scores).

We encountered some unexpected findings that raise important questions as to how to pursue this promising approach into human clinical trials. Clearly, the choice of specific antisense sequences is a crucial determinant of the ultimate success of targeted exon skipping. To date, specific AO sequences have been assessed for efficiency of exon skipping using cell-based experimental (*in vitro*) systems, with the optimal sequences then used for *in vivo* experiments. In studies presented here, antisense oligonucleotides directed against exon 6 were able to efficiently induce the desired exon 5 to 10 splicing *in vitro* but not *in vivo*. Our observations of discrepant outcomes for *ex vivo* and *in vivo* in the dystrophic dog tell us that we do not currently possess a reliable means of screening for sequences that induce efficient skipping of a particular exon in a particular mutational context. Data obtained from application of sequences as 2'O-MePs in primary myogenic cells or as PMOs incubated *ex vivo* with muscle fragments failed to predict the effects when PMO sequences were tested *in vivo*. The high percentage of in-frame products here might be related to nonsense-mediated decay of out-of-frame products or quality of RNA from cell culture; however, the *in vitro* experiments were consistent using three different concentrations (600, 60, and 30nM) with two different sequences (Ex6A and Ex6B). The results were confirmed by RT-PCR, immunohistochemistry, and complementary DNA sequences (see Fig 2; see Supplemental Fig 1). The *in vitro* effect of

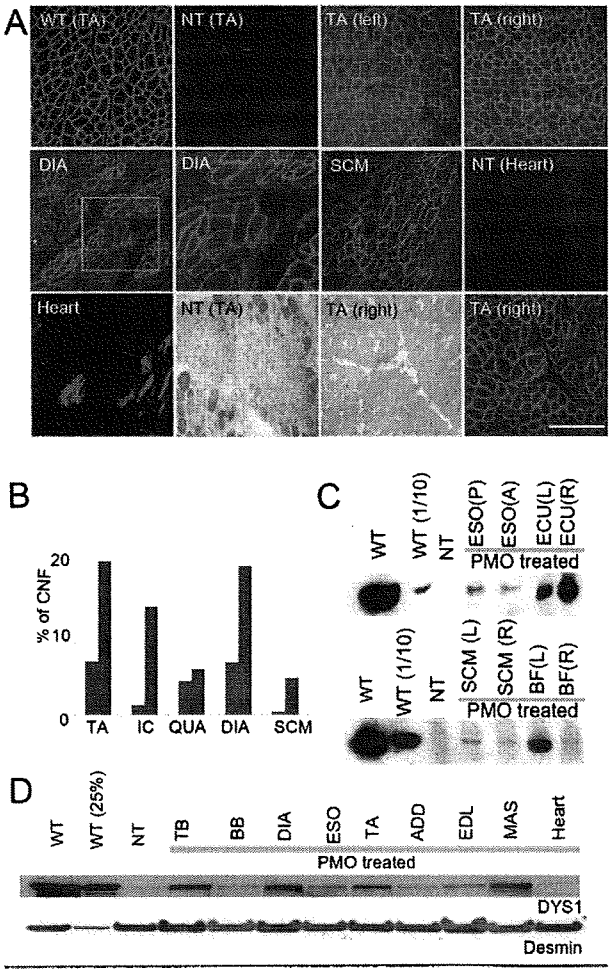

*Fig 4. Widespread dystrophin expression and improved histology by intravenous systemic delivery of cocktail morpholinos in canine X-linked muscular dystrophy (CXMD) dogs. (A) Dystrophin (DYS-1) staining and histology in bilateral tibialis anterior muscles (TA), diaphragm (DIA), sternocleidomastoid (SCM), and heart at 2 weeks after final injection after five weekly intravenous injections of 120mg/kg cocktail morpholinos containing Ex6A, Ex6B, and Ex8A (2001MA). Comparisons were made with TA from normal control animal (wild type [WT]) and from nontreated CXMD littermate (NT) tibialis anterior (TA) and heart. Intravenous morpholino treatment resulted in extensive, though variable, dystrophin production in multiple muscles, but with only limited evidence of rescue in heart (isolated cardiocytes). Paired dystrophin immunostaining and histology from treated dog (TA, bottom panels) showed improved histopathology relative to untreated littermate (NT TA) histology. Bars = 200μm, except for higher magnification picture of DIA and hearts (100μm). (B) Quantitation of centrally nucleated fibers (CNFs) in TA, intercostal (IC), quadriceps (QUA), diaphragm (DIA), and sternocleidomastoid (SCM) in treated dog (*blue bars; *2001MA) and untreated dog (red bars; 2008MA). (C) Western blotting analysis for detection of dystrophin at 2 weeks after final injection after 5 × weekly intravenous injections of 120mg/kg cocktail morpholinos containing Ex6A, Ex6B, and Ex8A (2001MA). Dystrophin rescue is variable with high expression in right extensor carpi ulnaris [ECU(R)] and left biceps femoris [BF(L)], and less in posterior [ESO(P)] or anterior esophagus [ESO(A)] and sternocleidomastoid (SCM). (D) Immunoblot analysis of dystrophin in intravenous morpholino-treated dog (2703MA; 7 × weekly dosing) and control animals (normal control [WT], nontreated [NT]). Desmin immunoblot is shown as a loading control. Dystrophin shows high levels (>25% control levels) in triceps brachii (TB), DIA, and masseter (MAS). ADD = adductor; BB = biceps brachii; EDL = extensor digitorum longus; MAS = masseter.*

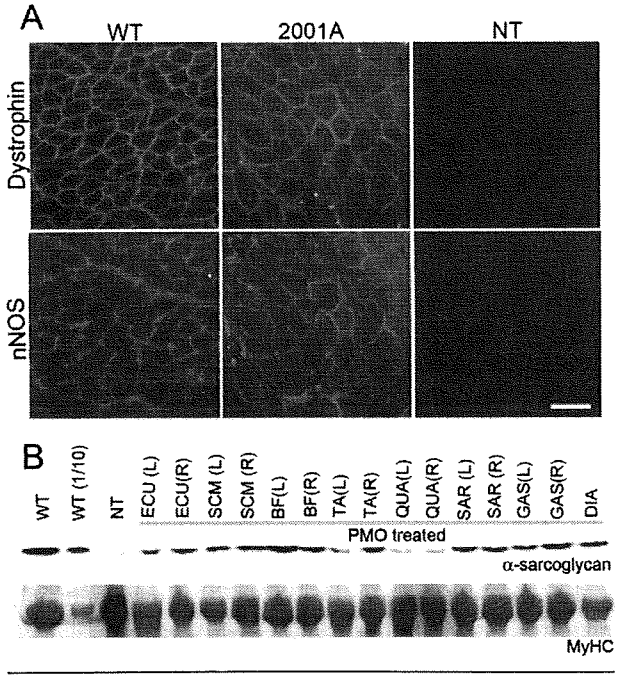

Fig 5. Recovery of localization and expression of dystrophin-associated proteins after systemic delivery of cocktail morpholinos to canine X-linked muscular dystrophy (CXMD) dogs. Neuronal nitric oxide synthase (nNOS) (A) and α-sarcoglycan (B) expression at 2 weeks after 5 × weekly 120mg/kg cocktail (2001MA) or 7 × weekly 200mg/kg cocktail morpholino injections (2703MA) to CXMD dogs. Recovery of nNOS expression at sarcolemma was observed by double immunofluorescence against dystrophin (DYS-1) and nNOS. Scale bar = 50μm. By immunoblot (B), α-sarcoglycan levels are increased in treated dog muscles, compared with untreated dystrophic controls (NT). Myosin heavy chain (MyHC) shown as a loading control. WT = wild-type normal control animals; WT(1/10) = wild-type (1/10 diluted samples, ie, 4μg loaded); NT = nontreated CXMD muscles (tibialis anterior); ECU = extensor carpi ulnaris; SCM = sternocleidomastoid; BF = biceps femoris; TA = tibialis anterior; QUA = quadriceps; SAR = sartorius; GAS = gastrocnemius; DIA = diaphragm; L = left side; R = right side.

the exon 6–specific sequence was, in addition, context dependent. For when transfected into wild-type Beagle myoblasts, the exon 8 AO pair again excised exons 8 and 9, whereas the exon 6–specific AO pair excised exons 6 and 9, leaving exons 7 and 8 in place (see Supplemental Fig 1). Thus, excision of exon 8 by the exon 6–specific sequences occurs only in the context of the mutant exon 7 splice site. Together, the differences between patterns of skipping *in vivo* versus *in vitro* and between wild-type versus mutant genotypes tell us that efficiency of skipping during transcription is dominated by variables other than the availability or otherwise of specific local sequence. Thus, it is prudent to consider testing of selected sequences in multiple systems with human dystrophin mRNA as the target before committing to a specific sequence for clinic trials.

We observed efficient skipping of exon 9, even though no antisense sequence targeted its removal in both wild-type and CXMD (see Figs 2 and 3), which is known as alternative splice site.[20] AOs targeting exon 8 have been reported to induce skipping of both exon 8 and 9 in human and in dog studies (see Figs 2 and 3).[10,21] It appears likely that the small size of intron 8 compared with intron 7 (1.1 vs 110Kb) predisposes to splicing of exon 8 to exon 9 before splicing to exon 7.

In the systemically treated dogs, we found widespread expression of dystrophin in all muscles analyzed but with considerable variation (see Fig 4). No difference in dystrophin expression between fiber types was evident

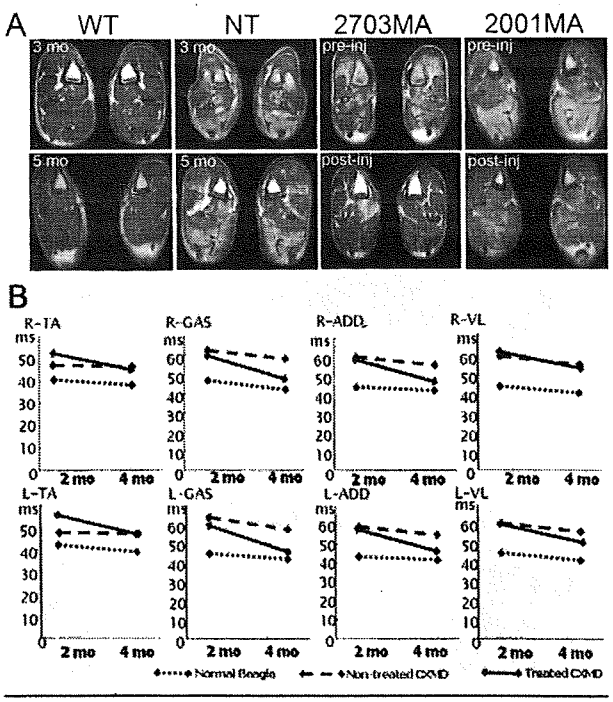

Fig 6. Amelioration of pathology and reduced inflammation signal in magnetic resonance imaging (MRI). T2-weighted MRI of hind legs at 1 week before initial injection (pre-inj) and at 2 weeks after final injection (post-inj) of 7 × weekly intravenous (IV) injection of 200mg/kg cocktail morpholinos (2703MA) or 5 × weekly IV injection of 120mg/kg cocktail morpholinos (2001MA). Age-matched untreated dogs (wild type [WT; normal control] and nontreated dystrophic control [NT]) are shown for comparison. (B) Changes of T2 value examined by MRI at 2 weeks after 7 × weekly 200mg/kg cocktail morpholino injections. Changes of T2 values in hind legs at 1 week before initial injection and at 2 weeks after final injection are shown. Intravenous morpholino treatment resulted in decreased T2 signal in all muscles examined. TA = tibialis anterior; GAS = gastrocnemius; ADD = adductor; VL = vastus lateralis. Dotted lines *represent normal Beagle;* dashed lines *represent nontreated canine X-linked muscular dystrophy (CXMD);* solid lines *represent treated CXMD.*

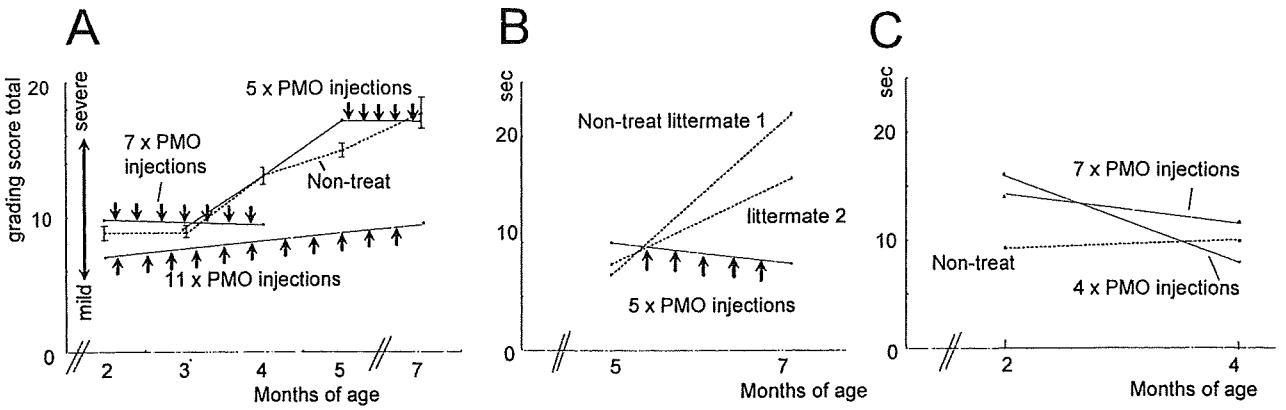

Fig 7. Stabilization of clinical symptoms by systemic morpholino treatment. (A) Combined clinical grading scores before (black lines) *and after starting treatment* (red lines) *of the three treated dogs. Clinical grades of gait disturbance, mobility disturbance, limb or temporal muscle atrophy, drooling, macroglossia, and dysphagia are scored as described in Materials and Methods. A series of untreated dogs (n = 6–13) was studied for comparison* (dashed line, *standard error bars). (B, C) Fifteen-meter timed running tests in treated dogs and untreated littermates. A canine X-linked muscular dystrophy (CXMD) dog treated from 5 to 7 months (2001MA) of age showed decreased timed 15m run after treatment, whereas untreated littermates showed slowed running ability (B). Similarly, two littermate dogs treated at 2 to 4 months of age (2703MA; 2702FA) showed quicker 15m times after treatment compared with nontreated littermate (C).*

(data not shown). Even contralateral muscles differed from one another, suggesting that variation in efficacy of dystrophin production is a reflection of transient sporadic events such as myopathic episodes or changes in vascularization or circulation rather than any intrinsic muscle-specific properties. Pathological stages of degeneration/regeneration may also be involved. Overall, most studies to date suggest that 10 to 20% normal dystrophin levels are needed to improve muscle function,[22,23] and the data on systemic morpholino-induced exon skipping presented here imply that some, but not all, muscle groups reached this therapeutic level.

Systemic delivery of morpholinos in CXMD dogs as in *mdx* mice induced only modest dystrophin production in the heart (see Fig 4).[19] The reason is not clear, but it has been suggested that dystrophic skeletal muscle fibers may give greater access to AOs because they have more "leaky" membranes than the smaller cardiac cells and because the syncytial structure of myofibers may permit wider diffusion of PMO molecules from each site of entry.[24] Cardiac ischemia, as indicated by abnormal Q-waves in CXMD,[25] may also limit access of AOs to cardiomyocytes. Some improvement in delivery has been reported with cell-penetrating peptide-tagged morpholinos, or use of microbubbles and ultrasound that may enhance uptake efficiency in the heart by facilitating penetration of cell membranes, although toxicity of these strategies is not clear.[26,27]

Considerable evidence for functional and histological improvement was seen in the three systemically treated dogs (see Figs 4–7). All were stabilized compared with their untreated littermates in motor function tests, general clinical condition, and serum creatine kinase levels. MRI images also showed reduction of T2-weighted signal, interpreted as a sign of diminished inflammation, after morpholino delivery (see Fig 6). However, longer-term experiments are required to investigate whether AOs can reduce infiltration by fibrofatty tissue and to what extent functional loss can be recovered.

Many DMD patients require two or more exons to be skipped to restore the reading frame. The data reported here are the first demonstrations of efficient skipping of multiple exons systemically through intravenous delivery. The dog model required skipping of two to three exons to restore the reading frame, and we were able to show efficient skipping of three exons by both intramuscular and intravenous delivery methods. Multiexon skipping has also been shown in *in vitro* cell cultures and in *mdx* mice by intramuscular injections.[8,28–30] Multiexon skipping increases the range of potentially treatable DMD patients and also raises the prospect of selecting the most functionally favorable in-frame dystrophins,[7] although skipping larger stretches of exons has yet not been achieved and currently may not be feasible. Specific morpholino cocktails able to treat a large proportion of DMD patients with optimized quasi-dystrophin production might be submitted for regulatory approval as a single "drug." For example, a cocktail of AOs targeting exons 45 to 55 would be applicable in up to 63% of patients with dystrophin deletions, and this specific deletion is associated with asymptomatic or mild BMD clinical phenotypes.[31,32]

This work was supported by the Foundation to Eradicate Duchenne, the Department of Defense CDMRP program (W81XWH-05-1-

0616 E.P.H.), the Jain Foundation (E.P.H.), the Crystal Ball of Virginia Beach (Muscular Dystrophy Association USA) (E.P.H.), the National Center for Medical Rehabilitation Research 5R24HD050846-02 (E.P.H.), the NIH Wellstone Muscular Dystrophy Research Centers IU54HD053177-01A1 (E.P.H.), and the Ministry of Health, Labor, and Welfare of Japan (Research on Nervous and Mental Disorders, 16B-2, 19A-7; Health and Labor Sciences, Research Grants for Translation Research, H19-translational research-003, Health Sciences Research Grants for Research on Psychiatry and Neurological Disease and Mental Health, H18-kokoro-019) (S.T.).

We thank Drs S. Duguez, J. Nazarian, H. Gordish-Dressman, Y. Aoki, T. Saito, K. Yuasa, N. Yugeta, S. Ohshima, Z.-H. Shin, MR. Wada, K. Fukushima, S. Masuda, K. Kinoshita, H. Kita, S. Ichikawa, Y. Yahata, T. Nakayama, A. Rabinowitz, and JR. Beauchamp for discussions and technical assistance.

References

1. Hoffman EP, Brown RH Jr, Kunkel LM. Dystrophin: the protein product of the Duchenne muscular dystrophy locus. Cell 1987;51:919–928.
2. Matsumura K, Campbell KP. Dystrophin-glycoprotein complex: its role in the molecular pathogenesis of muscular dystrophies. Muscle Nerve 1994;17:2–15.
3. Koenig M, Beggs AH, Moyer M, et al. The molecular basis for Duchenne versus Becker muscular dystrophy: correlation of severity with type of deletion. Am J Hum Genet 1989;45:498–506.
4. England SB, Nicholson LV, Johnson MA, et al. Very mild muscular dystrophy associated with the deletion of 46% of dystrophin. Nature 1990;343:180–182.
5. Dunckley MG, Manoharan M, Villiet P, et al. Modification of splicing in the dystrophin gene in cultured Mdx muscle cells by antisense oligoribonucleotides. Hum Mol Genet 1998;7:1083–1090.
6. van Deutekom JC, Janson AA, Ginjaar IB, et al. Local dystrophin restoration with antisense oligonucleotide PRO051. N Engl J Med 2007;357:2677–2686.
7. Yokota T, Duddy W, Partridge T. Optimizing exon skipping therapies for DMD. Acta Myol 2007;26:179–184.
8. Aartsma-Rus A, Janson AA, Kaman WE, et al. Antisense-induced multiexon skipping for Duchenne muscular dystrophy makes more sense. Am J Hum Genet 2004;74:83–92.
9. Sharp NJ, Kornegay JN, Van Camp SD, et al. An error in dystrophin mRNA processing in golden retriever muscular dystrophy, an animal homologue of Duchenne muscular dystrophy. Genomics 1992;13:115–121.
10. McClorey G, Moulton HM, Iversen PL, et al. Antisense oligonucleotide-induced exon skipping restores dystrophin expression in vitro in a canine model of DMD. Gene Ther 2006;13:1373–1381.
11. Shimatsu Y, Katagiri K, Furuta T, et al. Canine X-linked muscular dystrophy in Japan (CXMDJ). Exp Anim 2003;52:93–97.
12. Summerton J, Weller D. Morpholino antisense oligomers: design, preparation, and properties. Antisense Nucleic Acid Drug Dev 1997;7:187–195.
13. Yokota T, Takeda S, Lu QL, et al. A renaissance for anti-sense oligonucleotide drugs in neurology: exon-skipping breaks new ground. Arch Neurol 2009;66:32–38.
14. Jankowski RJ, Haluszczak C, Trucco M, Huard J. Flow cytometric characterization of myogenic cell populations obtained via the preplate technique: potential for rapid isolation of muscle-derived stem cells. Hum Gene Ther 2001;12:619–628.
15. Yokota T, Lu QL, Morgan JE, et al. Expansion of revertant fibers in dystrophic mdx muscles reflects activity of muscle precursor cells and serves as an index of muscle regeneration. J Cell Sci 2006;119:2679–2687.
16. Abramoff MD, Magelhaes PJ, Ram SJ. Image processing with ImageJ. Biophotonics Int 2004;11:36–42.
17. Araishi K, Sasaoka T, Imamura M, et al. Loss of the sarcoglycan complex and sarcospan leads to muscular dystrophy in beta-sarcoglycan-deficient mice. Hum Mol Genet 1999;8:1589–1598.
18. Shimatsu Y, Yoshimura M, Yuasa K, et al. Major clinical and histopathological characteristics of canine X-linked muscular dystrophy in Japan, CXMDJ. Acta Myol 2005;24:145–154.
19. Alter J, Lou F, Rabinowitz A, et al. Systemic delivery of morpholino oligonucleotide restores dystrophin expression bodywide and improves dystrophic pathology. Nat Med 2006;12:175–177.
20. Reiss J, Rininsland F. An explanation for the constitutive exon 9 cassette splicing of the DMD gene. Hum Mol Genet 1994;3:295–298.
21. Aartsma-Rus A, De Winter CL, Janson AA, et al. Functional analysis of 114 exon-internal AONs for targeted DMD exon skipping: indication for steric hindrance of SR protein binding sites. Oligonucleotides 2005;15:284–297.
22. Yoshimura M, Sakamoto M, Ikemoto M, et al. AAV vector-mediated microdystrophin expression in a relatively small percentage of mdx myofibers improved the mdx phenotype. Mol Ther 2004;10:821–828.
23. Liang KW, Nishikawa M, Liu F, et al. Restoration of dystrophin expression in mdx mice by intravascular injection of naked DNA containing full-length dystrophin cDNA. Gene Ther 2004;11:901–908.
24. Yokota T, Pistilli E, Duddy W, Nagaraju K. Potential of oligonucleotide-mediated exon-skipping therapy for Duchenne muscular dystrophy. Exp Opin Biol Ther 2007;7:831–842.
25. Yugeta N UN, Fujii Y, Yoshimura M, et al. Cardiac involvement in Beagle-based canine X-linked muscular dystrophy in Japan (CXMDJ): electrocardiographic, echocardiographic, and morphologic studies. BMC Cardiovasc Disord 2006;6:47.
26. Jearawiriyapaisarn N, Moulton HM, Buckley B, et al. Sustained dystrophin expression induced by peptide-conjugated morpholino oligomers in the muscles of mdx mice. Mol Ther 2008;16:1624–1629.
27. Vannan M, McCreery T, Li P, et al. Ultrasound-mediated transfection of canine myocardium by intravenous administration of cationic microbubble-linked plasmid DNA. J Am Soc Echocardiogr 2002;15:214–218.
28. Fall AM, Johnsen R, Honeyman K, et al. Induction of revertant fibres in the mdx mouse using antisense oligonucleotides. Genet Vaccines Ther 2006;4:3.
29. Aartsma-Rus A, Janson AA, van Ommen GJ, van Deutekom JC. Antisense-induced exon skipping for duplications in Duchenne muscular dystrophy. BMC Med Genet 2007;8:43.
30. Aartsma-Rus A, Kaman WE, Weij R, et al. Exploring the frontiers of therapeutic exon skipping for Duchenne muscular dystrophy by double targeting within one or multiple exons. Mol Ther 2006;14:401–407.
31. Nakamura A, Yoshida K, Fukushima K, et al. Follow-up of three patients with a large in-frame deletion of exons 45-55 in the Duchenne muscular dystrophy (DMD) gene. J Clin Neurosci 2008;15:757–763.
32. Beroud C, Tuffery-Giraud S, Matsuo M, et al. Multiexon skipping leading to an artificial DMD protein lacking amino acids from exons 45 through 55 could rescue up to 63% of patients with Duchenne muscular dystrophy. Hum Mutat 2007;28:196–202.

MECHANISMS OF DEVELOPMENT 126 (2009) 107–116

available at www.sciencedirect.com

ScienceDirect

journal homepage: www.elsevier.com/locate/modo

Reduced proliferative activity of primary POMGnT1-null myoblasts *in vitro*

Yuko Miyagoe-Suzuki[a,*], *Nami Masubuchi*[a,b], *Kaori Miyamoto*[a,b], *Michiko R. Wada*[a], *Shigeki Yuasa*[c], *Fumiaki Saito*[d], *Kiichiro Matsumura*[d], *Hironori Kanesaki*[e], *Akira Kudo*[e], *Hiroshi Manya*[f], *Tamao Endo*[f], *Shin'ichi Takeda*[a]

[a]*Department of Molecular Therapy, National Institute of Neuroscience, National Center of Neurology and Psychiatry, 4-1-1 Ogawahigashi, Kodaira, Tokyo 187-8502, Japan*
[b]*Molecular Embryology, Department of Biosciences, School of Science, Kitasato University, Kanagawa 228-8555, Japan*
[c]*Department of Ultrastructural Research, National Institute of Neuroscience, National Center of Neurology and Psychiatry, 4-1-1 Ogawahigashi, Kodaira, Tokyo 187-8502, Japan*
[d]*Department of Neurology and Neuroscience, Teikyo University School of Medicine, 2-11-1 Kaga, Itabashi-ku, Tokyo 173-8605, Japan*
[e]*Department of Biological Information, Tokyo Institute of Technology, Yokohama 226-8501, Japan*
[f]*Glycobiology Research Group, Tokyo Metropolitan Institute of Gerontology, Foundation for Research on Aging and Promotion of Human Welfare, 35-2 Sakaecho, Itabashi-ku, Tokyo 173-0015, Japan*

ARTICLE INFO

Article history:
Received 28 May 2008
Received in revised form
6 November 2008
Accepted 2 December 2008
Available online 16 December 2008

Keywords:
POMGnT1
Muscle–eye–brain disease
Satellite cells
Skeletal muscle
α-Dystroglycan
Glycosylation
Laminin

ABSTRACT

Protein O-linked mannose β1,2-*N*-acetylglucosaminyltransferase 1 (POMGnT1) is an enzyme that transfers *N*-acetylglucosamine to O-mannose of glycoproteins. Mutations of the *POMGnT1* gene cause muscle–eye–brain (MEB) disease. To obtain a better understanding of the pathogenesis of MEB disease, we mutated the *POMGnT1* gene in mice using a targeting technique. The mutant muscle showed aberrant glycosylation of α-DG, and α-DG from mutant muscle failed to bind laminin in a binding assay. *POMGnT1*$^{-/-}$ muscle showed minimal pathological changes with very low-serum creatine kinase levels, and had normally formed muscle basal lamina, but showed reduced muscle mass, reduced numbers of muscle fibers, and impaired muscle regeneration. Importantly, *POMGnT1*$^{-/-}$ satellite cells proliferated slowly, but efficiently differentiated into multinuclear myotubes *in vitro*. Transfer of a retrovirus vector-mediated *POMGnT1* gene into *POMGnT1*$^{-/-}$ myoblasts completely restored the glycosylation of α-DG, but proliferation of the cells was not improved. Our results suggest that proper glycosylation of α-DG is important for maintenance of the proliferative activity of satellite cells *in vivo*.

1. Introduction

POMGnT1 is the glycosyltransferase that catalyzes the transfer of N-acetylglucosamine (GlcNAc) to O-mannose of glycoproteins, the second step of Ser/Thr O-mannosylation (Yoshida et al., 2001; reviewed in Endo and Toda, 2003). Mutations in the *POMGnT1* gene cause muscle–eye–brain (MEB) disease, a rare autosomal recessive disorder characterized by congenital muscular dystrophy with elevated serum creatine kinase (CK) levels, severe visual failure, and gross mental retardation (Yoshida et al., 2001).

* *Corresponding author.* Tel.: +81 42 346 1720; fax: +81 42 346 1750.
E-mail address: miyagoe@ncnp.go.jp (Y. Miyagoe-Suzuki).
0925-4773/$ - see front matter © 2008 Elsevier Ireland Ltd. All rights reserved.
doi:10.1016/j.mod.2008.12.001

α-Dystroglycan (α-DG) is a heavily glycosylated glycoprotein and a well-known substrate of POMGnT1. Dystroglycan is encoded by a single gene (*DAG1*) and is cleaved into two proteins, α-dystroglycan (α-DG) and β-dystroglycan (β-DG), by posttranslational processing (Ibraghimov-Beskrovnaya et al., 1992). DGs are central components of the dystrophin–glycoprotein complex (DGC) at the sarcolemma, and α-DG was shown to serve as a cell surface receptor for laminin (Ibraghimov-Beskrovnaya et al., 1992), agrin (Gee et al., 1994; Campanelli et al., 1994), perlecan (Peng et al., 1998; Kanagawa et al., 2005), and neurexin (Sugita et al., 2001). In skeletal muscle, the laminin-α-DG linkage is thought to be critical for plasma membrane stability (recently reviewed in Kanagawa and Toda 2006). In MEB muscle, the α-DG core protein is preserved but hypo-glycosylated, and α-DG prepared from the muscle fails to bind laminin *in vitro* (Michele et al., 2002). Therefore, it is proposed that the disruption of the α-DG-laminin linkage is the main pathomechanism of dystrophic changes seen in MEB muscle.

To further elucidate the molecular pathogenesis of MEB disease, we generated *POMGnT1*-knockout mice using a gene targeting technique, and examined the mutant skeletal muscle. During our experiments, Liu et al. reported the generation of POMGnT1-deficient mice (Liu et al., 2006). The report showed severe muscle pathology, but the mechanism by which POMGnT1 deficiency causes muscle phenotype was not clearly shown. In this report, we report that POMGnT1-deficient mice show remarkably minimal signs of muscle degeneration and regeneration, but also show small muscle mass, reduced numbers of muscle fibers, and impaired muscle regeneration. POMGnT1-deficient myoblasts proliferate poorly *in vitro*. The proliferation was not improved by retrovirus vector-mediated *POMGnT1* expression in *POMGnT1*$^{-/-}$ myoblasts, suggesting that α-DG–laminin interaction *in vivo* is important for maintenance of the proliferative activity of satellite cells.

2. Results

2.1. *Inactivation of the POMGnT1 gene in mice*

We mutated the *POMGnT1* gene by replacing exon 18 with a neomycin-resistance gene in mouse ES cells (depicted in Fig. 1). Two ES clones successfully entered the germline. Although there was no evidence of embryonic lethality, more than 60% of the homozygotes died within 3 weeks of birth. Survivors were smaller than their wild-type littermates (Fig. 3A) throughout life, but most of them had a normal life span. We confirmed that the *POMGnT1*$^{-/-}$ mice completely lacked the POMGnT1 enzyme activity (Fig. 2A). A monoclonal antibody, VIA4-1, that reacts with the suger moiety of α-DG gave no signal in either *POMGnT1*$^{-/-}$ brain (Fig. 2B) or muscle (data not shown). A polyclonal antibody against α-DG core protein revealed that the *POMGnT1*$^{-/-}$ brain expresses approximately 80 kDa α-DG protein, which is much smaller than that seen in the wild-type brain (ca. 110 kDa) (Fig. 2C). We next examined whether α-DG in *POMGnT1*$^{-/-}$ brain binds laminin. Wheat germ agglutinin (WGA)-enriched brain protein from control and *POMGnT1*$^{-/-}$ mice was separated on SDS–PAGE gels, blotted onto a PVDF membrane, incubated with EHS laminin, and then bound laminin was detected by an anti-laminin antibody. α-DG in *POMGnT1*$^{-/-}$ brain failed to bind to laminin (Fig. 2D).

2.2. *POMGnT1*$^{-/-}$ *muscle shows very mild dystrophic changes*

Immunohistochemistry of cross-sections of tibialis anterior (TA) muscles showed that dystrophin and other members of the DGC complex were normally expressed at the sarcolemma of *POMGnT1*$^{-/-}$ muscle (Fig. 3 and Table 1). Laminin α2 chain was detected around POMGnT1$^{-/-}$ muscle fibers. On H.E.-stained cross-sections, surprisingly, the POMGnT1$^{-/-}$ muscle showed almost normal morphology. Central nucleation of myofibers indicates regeneration events in the past. In the TA muscles of 4-week-old wild-type mice, 0.25% of myofibers were centrally nucleated. In POMGnT1$^{-/-}$ mice, 0.28% of the myofibers had central nuclei. In contrast, ca. 40–50% of myofibers of age-matched mdx mice were centrally nucleated. Even at 24 months of age, the percentage of centrally nucleated myofibers was lower (3.6%) in POMGnT1$^{-/-}$ TA muscle, compared with age-matched wild-type TA muscle (9.0%). POMGnT1$^{-/-}$ TA muscle also lacked other signs of degeneration and regeneration. Electrophoresis of muscle extracts on glycerol SDS–PAGE gels showed no difference in MyHC isoform composition of quadriceps and gastrocnemius muscles between POMGnT1$^{-/-}$ and wild-type littermates (data not shown). In both wild-type and POMGnT1$^{-/-}$ muscle, the muscle basal lamina was normally formed (Supplementary Fig. 1). Electron microscopy also showed that the sarcomere structures are almost normal in POMGnT1$^{-/-}$ mice. We next examined the serum creatine kinase (CK) levels, an index of on-going muscle damage, in wild-type, POMGnT1$^{-/-}$, and age-matched mdx mice (Fig. 5). The serum CK levels of 5- to 20-week-old POMGnT1$^{-/-}$ mice were slightly higher (av. 586 U/L, $n = 10$) ($p < 0.05$) than those of wild-type littermates (less than 100 U/L, $n = 4$), but were much lower than those of mdx mice (more than 5000 U/L, $n = 3$, $p < 0.01$). The serum CK levels of 2-year-old POMGnT1$^{-/-}$ mice were still low (less than 300 U/L, $n = 4$).

2.3. *Repetitive muscle injury causes more fibrosis and fatty infiltration in POMGnT1*$^{-/-}$ *than in WT TA muscle*

Dystroglycans expressed on the cell membrane of satellite cells are proposed to play an important role in muscle regeneration (Cohn et al., 2002). In addition, the average size of *POMGnT1*$^{-/-}$ myofibers was smaller than those of wild-type myofibers (Fig. 4). Moreover, the number of myofibers is reduced in *POMGnT1*$^{-/-}$ skeletal muscle of neonatal and adult POMGnT1 mice, suggesting proliferation defect of *POMGnT1*$^{-/-}$ myoblasts (Fig. 4). To test the hypothesis, we damaged *POMGnT1*$^{-/-}$ TA muscle by cardiotoxin (CTX) and examined their regeneration. After single cardiotoxin injection, *POMGnT1*$^{-/-}$ muscle regenerated well like wild-type (data not shown). Next, we injected CTX into TA muscles of *POMGnT1*$^{-/-}$ and heterozygous littermates three times at intervals of 2 weeks, or 1 week interval, and examined the muscle. We summarized the results in Fig. 6. *POMGnT1*$^{-/-}$ muscle showed more fibrosis and

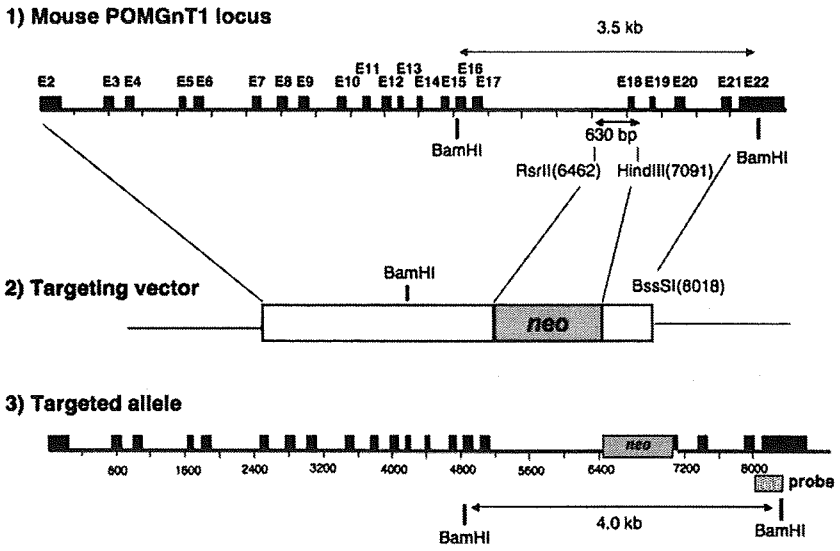

Fig. 1 – Targeted disruption of the mouse POMGnT1 gene in embryonic stem (ES) cells. The successfully targeted allele lacks a 630 bp-genome fragment containing exon 18, and instead has a *neo* resistance gene. Recombination in ES cells was confirmed by Southern blotting with the probe shown by a shaded box. The nucleic acid numbers are from AB053221 in GenBank.

fatty infiltration, which is a sign of inefficient muscle regeneration, than *POMGnT1*$^{+/-}$ muscle. Together with reduced numbers of myofibers in muscle, the results suggest that the function of satellite cells in *POMGnT1*$^{-/-}$ skeletal muscle is impaired.

2.4. *Defective proliferative activity of POMGnT1*$^{-/-}$ *myoblasts*

We next tested activation and proliferation of satellite cells on living myofibers isolated from wild-type and *POMGnT1*$^{-/-}$

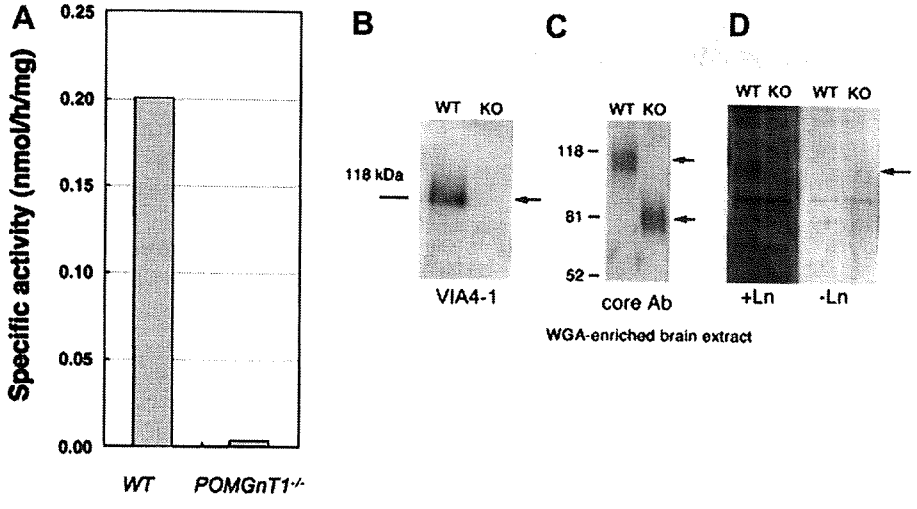

Fig. 2 – *POMGnT1*$^{-/-}$ mice show undetectable POMGnT1 enzyme activity and aberrant glycosylation of α-dystroglycan (α-DG) in *POMGnT1*$^{-/-}$ mice. (A) The amount of POMGnT1 activity is based on the amount of [^{3}H]GlcNAc transferred from UDP-GlcNAc to mannosyl peptide. The reaction product was purified by reverse-phased HPLC, and the radioactivity was measured. (B) Wheat germ agglutinin (WGA) agarose-enriched brain extracts from wild-type (WT) or *POMGnT1*$^{-/-}$ (KO) mice were resolved on a 7.5% SDS–PAGE gel, transferred to a PVDF membrane, and probed with anti-α-DG antibody, VIA4-1, which recognizes glycosylated α-DG. (C) The blot was incubated with polyclonal antibodies specific for α-DG core protein. The antibody detected ~110 kDa bands in wild-type brain extract, and 80 kDa bands in the brain extract of *POMGnT1*$^{-/-}$ mice. (D) Laminin overlay assay showing that α-DG in *POMGnT1*$^{-/-}$ brain does not bind laminin *in vitro*. +Ln, laminin was incubated with the blotted membrane. –LN, without laminin.

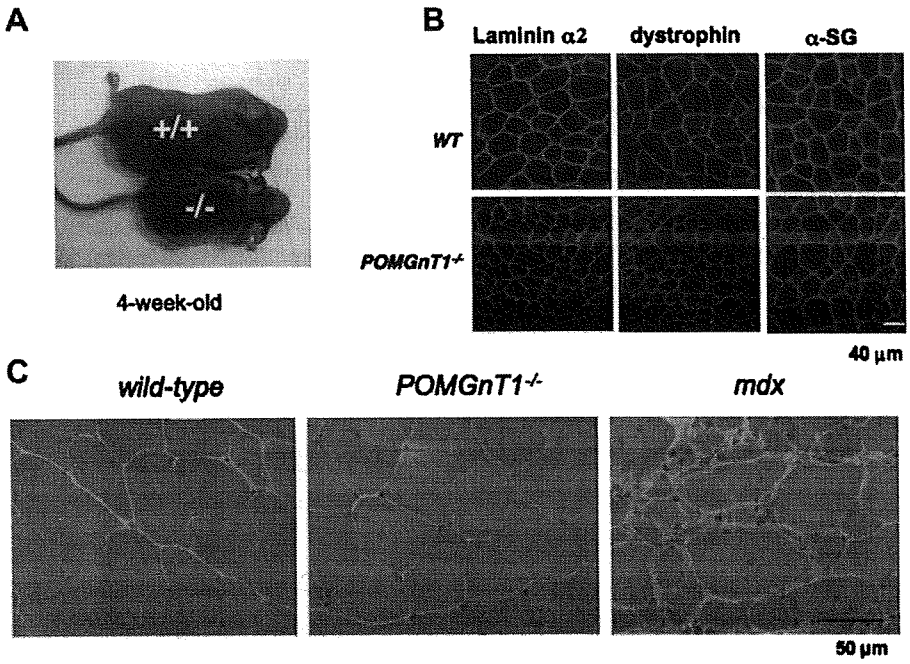

Fig. 3 – Remarkably mild dystrophic phenotypes of POMGnT1$^{-/-}$ muscle. (A) A photo of representative 4-week-old wild-type (+/+) and POMGnT1$^{-/-}$ (–/–) mice. POMGnT1$^{-/-}$ mice are smaller than wild-type littermates. (B) Immunohistochemistry of wild-type (+/+) and POMGnT1-knockout (–/–). Laminin α2 chain, dystrophin, and α-sarcoglycan are expressed normally on the sarcolemma of POMGnT1$^{-/-}$ muscle. (C) Representative H.E. staining of cross-sections of the TA muscles from POMGnT1$^{-/-}$, wild-type, and age-matched dystrophin-deficient *mdx* mice. POMGnT1$^{-/-}$ muscle shows minimal signs of degeneration and regeneration.

Table 1 – Summary of immunohistochemistry of hind-limb muscles of wild-type (WT) POMGnT1$^{-/-}$, and mdx mice.

	WT	POMGnT1$^{-/-}$	*mdx*
Laminin α2 chain	+	+	+
Dystrophin	+	+	–
α-Dystroglycan (VIA4-1)	+	–	±
Dystroglycan (core protein)	+	+	±
β-Dystropglycan	+	+	±
α-Sarcoglycan	+	+	±
α-Syntrophin	+	+	±
nNOS	+	+	±
Aquaporin 4	+	+	±
Integrin α7	+	+	++
Integrin β1	+	+	++

+, expressed; –, absent; ±, down-regulated; ++, up-regulated.

mice (Fig. 7). Three days after plating of single myofibers on Matrigel-coated 24-well plates in growth medium, the numbers of detached satellite cells (activated and proliferating satellite cells) were counted. In both extensor digitorum longus (EDL) (fast twitch muscle) and soleus (slow twitch muscle) muscles, the numbers of activated satellite cells and proliferating satellite cells (myoblasts) around the parental myofiber were more numerous in wild-type than in POMGnT1$^{-/-}$ (Fig. 7). Furthermore, wild-type satellite cells migrate a little faster than POMGnT1$^{-/-}$ satellite cells on transwells (data not shown), although the difference was little. Therefore, our results suggest that POMGnT1$^{-/-}$ satellite cells are activated more slowly or proliferate more slowly than wild-type. We next isolated satellite cells from hind limb muscles of wild-type and POMGnT1$^{-/-}$ mice by a monoclonal antibody, SM/C-2.6, and flow cytometry (Fukada et al., 2007), and examined their proliferation rate. The total yield of satellite cells per gram of POMGnT1$^{-/-}$ muscle tissue was nearly the same as those of wild-type muscle (data not shown). The percentage of Ki67-positive satellite cells (cycling cells) was less than 1% in both wild-type and POMGnT1$^{-/-}$ mice, indicating that they are in the quiescent stage (data not shown). However, after plating wild-type and POMGnT1$^{-/-}$ satellite cells onto Matrigel-coated 6-well plates at the same density, we found that POMGnT1$^{-/-}$ satellite cells grew poorly in growth medium (Fig. 7B). The timing of activation (i.e. enlargement of the cytoplasm and MyoD expression) was the same with that of wild-type satellite cells (data not shown). Next, we cultured satellite cells on Matrigel-coated 24-well-plates in growth medium, and the cells growth was evaluated by MTT assay 1, 2, 3, 4, 5, 6, and 7 days after plating (Fig. 8). The assay revealed that wild-type myoblasts proliferated more rapidly than POMGnT1$^{-/-}$ myoblasts *in vitro*. POMGnT1$^{-/-}$ myoblasts fused normally to form multinucleated myotubes in differentiation conditions like the wild-type (data not shown), and there was no significant difference in the fusion index between wild-type (45%) and POMGnT1$^{-/-}$ myoblasts (40%) ($p > 0.05$).

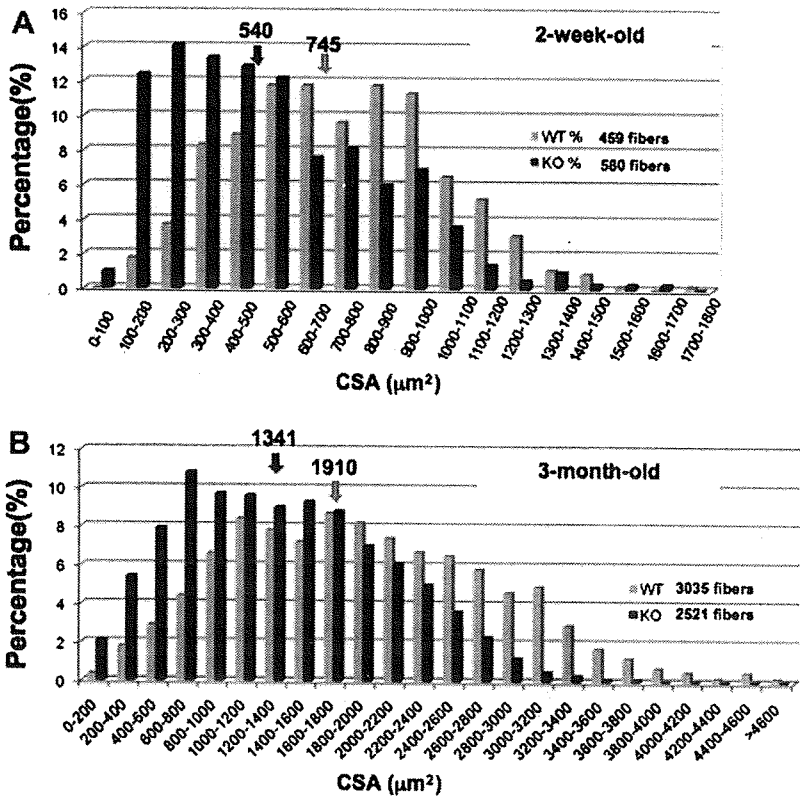

Fig. 4 – Cross-sectional area (CSA) of myofibers of POMGnT1$^{-/-}$ and wild-type mice. (A) A representative frequency graph of CSA of rectus femoris muscles from 2-week-old POMGnT1$^{-/-}$ (blue) and wild-type (light blue) littermates. The cross-sections were stained with anti-laminin α2 chain antibody. CSA of 459 POMGnT1$^{-/-}$ fibers and 580 wild-type fibers were measured and plotted. X-axis indicates CSA (μm^2), and Y-axis indicates percentages. Arrows indicate the averages. The total number of myofibers was also reduced in POMGnT1$^{-/-}$ mice (4169 vs. 3510). (B) The CSA of myofibers in TA muscles from 3-month-old POMGnT1$^{-/-}$ (blue) and wild-type (light blue) male mice was plotted as in (A)). In (B), almost all myofibers were measured (3035 fibers in wild-type TA and 2521 fibers in POMGnT1$^{-/-}$ TA).

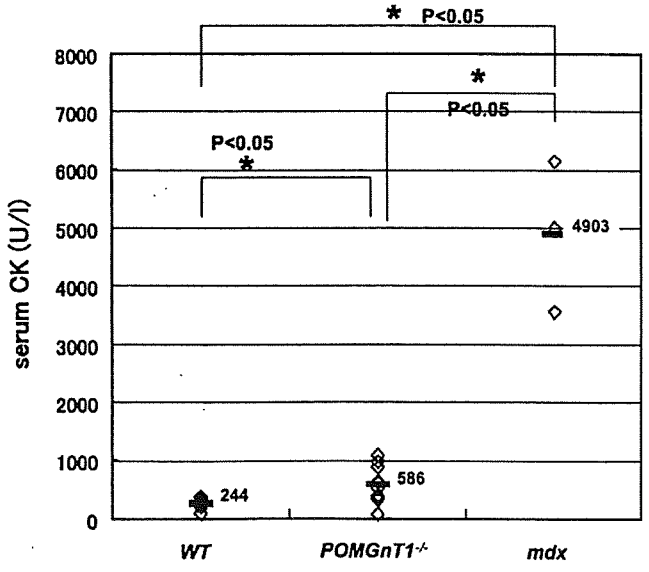

Fig. 5 – Serum CK levels of POMGnT1$^{-/-}$, wild-type, and *mdx* mice. Serum CK levels of 7–20 weeks old POMGnT1$^{-/-}$ mice (5 males and 5 females), wild-type littermates (3 males and 1 female), and three male *mdx* mice were measured and plotted on the graph with average. $^*p < 0.05$.

Next, we examined whether restoration of the expression of the POMGnT1 gene in mutant myoblasts improved their proliferation. To this end, we prepared a retrovirus vector, (pMX-POMGnT1-IRES-GFP) expressing human POMGnT1 and GFP. The recombinant retrovirus successfully restored O-mannosyl glycosylation of α-DG (Fig. 7A), but the proliferation rate was not changed (Fig. 8B).

2.5. *Cell growth signaling in POMGnT1$^{-/-}$ myoblasts*

It was previously reported that enhanced expression of α7β1 integrin ameliorates the development of muscular dystrophy and extends longevity in α7BX2-*mdx/utr*($^{-/-}$) transgenic mice (Burkin et al., 2001; Burkin et al., 2005), suggesting that integrin compensates for the function of α-DG in skeletal muscle to some extent. Therefore, we next examined the expression of β1-integrin in wild-type and POMGnT1$^{-/-}$ myoblasts (Supplementary Fig. 1). Western blotting, however, showed no difference between the β1-integrin protein levels in wild-type and POMGnT1$^{-/-}$ myoblasts (Supplementary Fig. 1A). Furthermore, FACS analysis showed similar levels of β1 integrin expression on the surfaces of myoblasts (Supplementary Fig. 1B). We then examined the activation levels of Akt and GSK-3β, both of which are involved in the

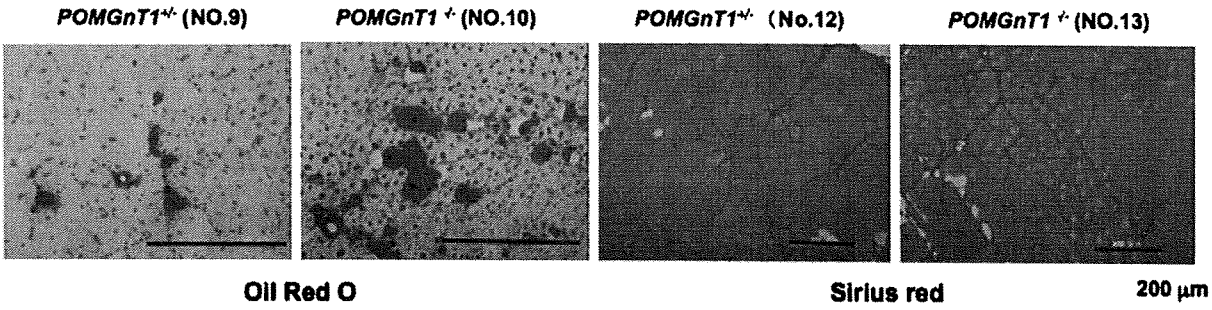

	genotype	sex	age	CTX interval(x3)	Fatty infiltration	Fibrosis
1	+/-	F	3M	2w	-	-
2	+/-	F	3M	2w	-	-
3	+/-	F	3M	2w	-→+	-→+
4	+/-	F	3M	2w	+	-→+
5	-/-	M	3M	2w	+	-→+
6	-/-	F	3M	2w	++	-→+
7	+/-	F	11M	1w	+	+
8	-/-	F	8.5M	1w	+	++
9	+/-	F	8.5M	1w	+	-→+
10	-/-	F	8.5M	1w	+→++	+→++
11	+/-	M	8.5M	1w	+	+
12	+/-	M	8.5M	1w	++	+
13	-/-	M	8.5M	1w	++	++

Fig. 6 – Impaired muscle regeneration of POMGnT1$^{-/-}$ mice. upper panel: representative Oil red O-stained or Sirius red-stained cross-sections of TA muscles of POMGnT1$^{-/-}$(−/−) and POMGnT1$^{+/-}$ (+/−) mice after three rounds of degeneration/regeneration evoked by cardiotoxin injection. One week after the last CTX injection, TA muscles were dissected, sectioned by a cryostat, fixed, and stained. lower table: Summary of fatty infiltration and fibrosis in regenerated muscles. CTX was injected into TA muscles three times with 2 weeks interval (2w) or 1 week interval (1w). The age at the first injection was shown. (−), well regenerated with minimal changes. (−→+), sporadic fatty regeneration or slight fibrosis between fibers. (+), mild fatty infiltration or mild fibrosis. (++), dense fatty infiltration or extensive fibrosis. F, female; M, male.

regulation of cell survival and proliferation. The levels of phosphorylation of these two kinases in POMGnT1$^{-/-}$ myoblasts were similar with those in wild-type myoblasts (Supplementary Fig. 1C). Consistent with these observations, TUNEL assay indicated that apoptosis is rare both in POMGnT1$^{-/-}$ and wild-type muscles (data not shown).

3. Discussion

In this study, we showed that in spite of mild muscle degeneration, the POMGnT1$^{-/-}$ satellite cells have much lower proliferative activity than wild-type satellite cells. The defect was not recovered by restoration of normal glycosylation of α-DG in mutant satellite cells. Together with the reduced sizes and the reduced numbers of myofibers of neonatal and adult POMGnT1$^{-/-}$ mice, these observations suggest that deficiency of POMGnT1 enzymatic activity impairs the functions of satellite cells.

3.1. *Two mouse models of muscle–eye–brain (MEB) disease*

Our POMGnT1$^{-/-}$ mice are the second mouse model of MEB disease. The first one was generated by gene trapping with a retroviral vector inserted into the second exon of the mouse POMGnT1 locus (Liu et al., 2006). As described in the literature, the phenotype is similar to ours with some differences. Our model shows much milder muscle phenotypes than the previously reported model, but also shows much a lower survival rate in the postnatal stage than the first model does. This would be due to more severe developmental abnormalities of the central nervous system of our mouse model, including disruption of the glia limitans, abnormal migration of neurons, and reactive gliosis in the cerebral cortex (manuscript in preparation), although these are also observed in the first model (Yang et al., 2007; Hu et al., 2007).

Mutation of the POMGnT1 gene is the cause of muscle–eye–brain disease (MEB) (Yoshida et al., 2001), which is characterized by severe congenital muscular dystrophy (Voit and Tome, 2004). Although glycosylation of α-DG was completely perturbed in our model, the POMGnT1$^{-/-}$ muscle showed only marginal pathological changes. Furthermore, POMGnT1$^{-/-}$ muscle showed normally formed muscle basal lamina on EM. These observations are in sharp contrast to the condition in humans. One possibility is that in the mouse, molecules other than α-DG are involved in the linkage of the sarcolemma with the extracellular matrix proteins, stabilizing the plasma membrane. As a candidate molecule, we examined β1-integrin expression in POMGnT1$^{-/-}$ muscle, but found that the level was not up-regulated. Therefore, the mechanism that explains this discrepancy remains to be clarified in a future study.

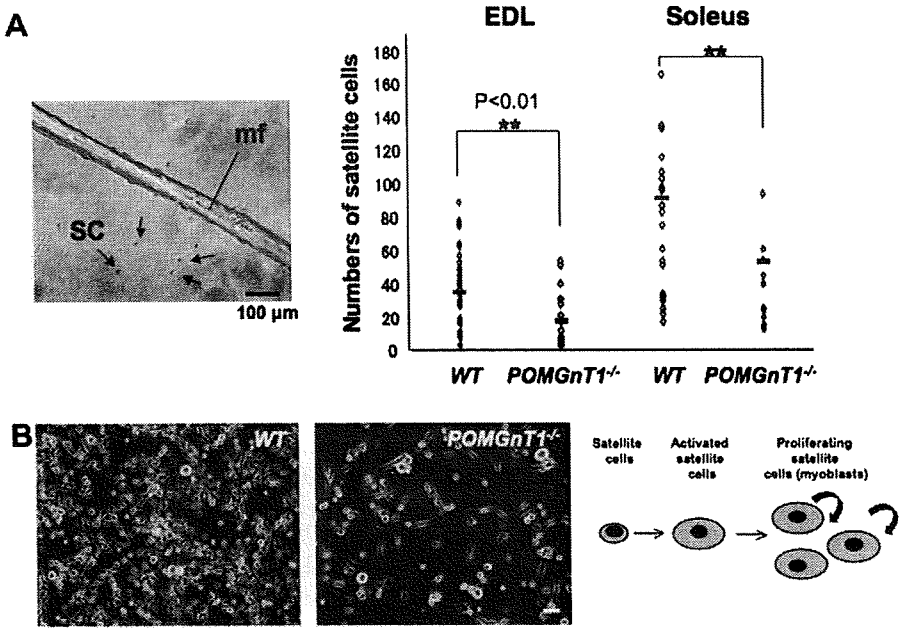

Fig. 7 – Activation and proliferation of satellite cells from WT and POMGnT1$^{-/-}$ mice. (A) Isolated myofibers were plated on Matrigel-coated 24 well-plates at one myofiber per well. Three days later, activated satellite cells (SC, arrows) around the parental fiber (mf) were counted and plotted. Small horizontal bars indicate the average number of activated/proliferating satellite cells originating from a myofiber from three independent experiments. Student's t-test. "$p < 0.01$ (wild-type vs. POMGnT1$^{-/-}$ mice). (B) Satellite cells from WT and POMGnT1$^{-/-}$ mice 7 days after plating onto Matrigel-coated 24-well-plates at 2.5×10^3 cells/well. Scale bar, 100 μm.

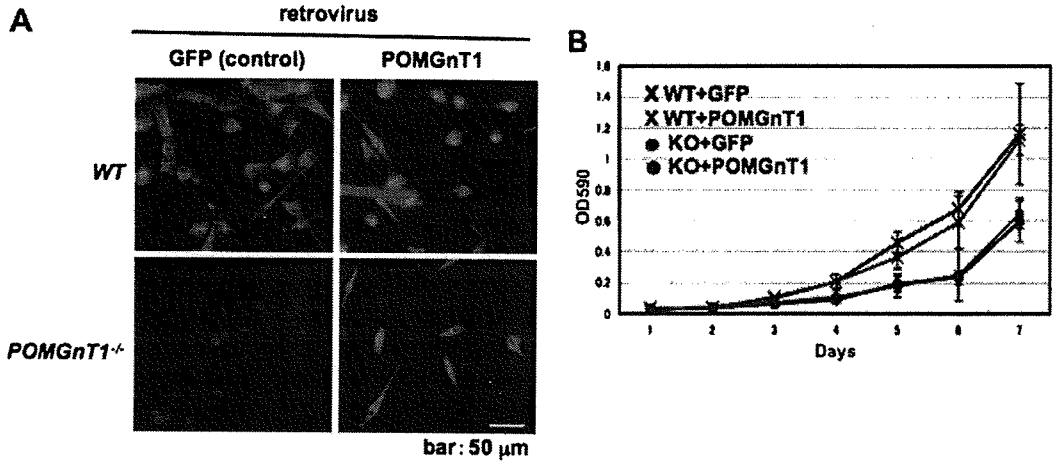

Fig. 8 – Restoration of POMGnT1 expression in POMGnT1$^{-/-}$ myoblasts does not improve proliferation of cells. (A) Wild-type (WT) and POMGnT1$^{-/-}$ myoblasts were transduced with a retrovirus expressing both POMGnT1 and GFP (POMGnT1) or only GFP (GFP, control), and the FACS-purified transduced cells were stained with anti-glycosylated α-DG monoclonal antibody (VIA4-1; red) and DAPI (Nucleus, blue). Note that the glycosylation of α-DG in POMGnT1$^{-/-}$ myoblasts was completely recovered by a retrovirus vector expressing POMGnT1. (B) MTT assay of wild-type (WT) and POMGnT1$^{-/-}$ myoblasts after infection with retrovirus vectors. Impaired proliferation of POMGnT1$^{-/-}$ myoblasts was not recovered by retrovirus-mediated expression of POMGnT1. Representative data of three independent experiments are shown.

3.2. *Null mutation in POMGnT1 reduces proliferative activity of muscle satellite cells*

POMGnT1$^{-/-}$ myoblasts proliferate poorly *in vitro*. This observation suggested that the proliferation of myoblasts is stimulated by growth signals *via* laminin-α-DG interaction. However, retrovirus vector-mediated gene transfer of the *POMGnT1* gene, which successfully restored O-mannosyl glycosylation of α-DG, did not restore the proliferation activity of the POMGnT1$^{-/-}$ myoblasts. DMD myoblasts proliferate poorly and quickly reach senescence. The impaired proliferation activity has been ascribed to repeated activation of

satellite cells due to repetitive cycles of muscle degeneration and regeneration (Blau et al., 1983). In contrast, *POMGnT1*$^{-/-}$ muscle lacks signs of active regeneration. Therefore, the reduced proliferation activity of *POMGnT1*$^{-/-}$ mouse myoblasts is not likely due to excessive cell division of satellite cells. Rather, it is likely that α-DG-laminin interaction in the niche, i.e. beneath the basal lamina of skeletal muscle myofibers, is important for maintenance of proliferative activity of satellite cells. However, the possibility that POMGnT1-deficiency causes aberrant glycosylation of molecules other than α-DG should be also tested.

Our results also suggested that the lack of α-DG-laminin interaction resulted in reduced numbers of muscle fibers (hypoplasia). Importantly, we found that myofibers of older *POMGnT1*$^{-/-}$ mice tend to be hypertrophied (Supplementary Fig. 2). *POMGnT1*$^{-/-}$ muscle might compensate the muscle power by hypertrophy of the myofibers. This is consistent with our observation that *POMGnT1*$^{-/-}$ muscle increases its mass in an overload model (unpublished data). Importantly, recent studies suggest that this process is satellite cell-independent (Sandri M., 2008).

Recently, Liu et al. showed that over-expression of integrin α7β1 in C2C12 myoblasts promoted proliferation of the cells (Liu et al., 2008). Importantly, however, we did not observe up-regulation of integrin α7β1 expression in *POMGnT1*$^{-/-}$ satellite cells. These observations suggest that dystroglycans and integrins have distinct roles in the regulation of muscle satellite cells.

In summary, we generated POMGnT1-null mice. The mice showed low serum creatine kinase levels and minimal signs of muscle degeneration and regeneration. Nonetheless, *POMGnT1*$^{-/-}$ muscle showed the reduction in the size and the number of myofibers. Furthermore, repeated injection of cardiotoxin showed impaired muscle regeneration in *POMGnT1*$^{-/-}$ mice. *POMGnT1*$^{-/-}$ myoblasts proliferated poorly *in vitro*. Over-expression of protein restored glycosylation of α-DG, but did not improve the proliferation of *POMGnT1*$^{-/-}$ myoblasts at all. Collectively, our results suggest that POMGnT1 enzymatic activity is important for maintenance of the proliferative activity of satellite cells *in vivo*.

4. Experimental procedures

4.1. Generation of *POMGnT1*$^{-/-}$ mice

The targeting strategy in ES cells is depicted in Fig. 1. Genomic DNA (8.6 kb) covering almost the entire *POMGnT1* gene was isolated from 129/SvJ mice by using two specific primers: m1F2 primer, 5′-gat tcc tga agt cat gga ctg gc-3′ and m1B5, 5′-tct aaa ggt ctc tgt gtg agt ctg tca g-3′. The PCR product was then cloned into a TOPO TA cloning vector (Invitrogen, Carlsbad, CA) and sequenced (AB053221). To construct the targeting vector, a 630-bp RsrII-Hind III fragment, containing exon18 was replaced with a *neo* expression cassette (Stratagene) (Fig. 1). Electroporation and screening of ES cells (129Svev origin) were performed by Ingenious Targeting Laboratory, Inc. (Stony Brook, NY). Homologous recombination in ES cells was confirmed by Southern blotting. Two independent positive ES clones were injected into C57BL/6 blastocysts, which gave rise to offspring carrying the mutated allele. Genotyping of the mice was done by PCR. One primer set is designed to amplify exon 18: F2, 5′-cag cag ttt cct tcc ttc taa ccc-3′ and B4, 5′-att tgg tct ggt ccc ttg gct c-3′ (278 bp). *Neo* primers were used to amplify the *neo* resistance gene, and thereby detect the mutant allele: neo-F, 5′-agg cta ttc ggc tat gac tgg g-3′, and neo-R, 5′-tac ttt ctc ggc agg agc aag gtg-3′ (288 bp). Dystrophin-deficient *mdx* mice of C57BL/6 genetic background were provided by T. Sasaoka at the National Institute for Basic Biology, Japan. The Experimental Animal Care and Use Committee of the National Institute of Neuroscience approved all experimental protocols.

4.2. *POMGnT1* enzymatic activity

Brains were obtained from 8-week-old mice and homogenized with nine volumes (weight/volume) of 10 mM Tris–HCl, pH 7.4, 1 mM EDTA, and 250 mM sucrose. After centrifugation at 900*g* for 10 min, the supernatant was subjected to ultracentrifugation at 100,000*g* for 1 h. The precipitates were used as the microsomal membrane fraction. The protein concentration was determined by BCA assay (Pierce, Rockford, IL). The enzymatic activity assay measured the amount of [^{3}H]GlcNAc transferred to a mannosyl peptide (Akasaka-Manya et al., 2004). Briefly, a reaction mixture containing 140 mM Mes buffer (pH 7.0), 1 mM UDP-[^{3}H]GlcNAc (80,000 dpm/nmol, PerkinElmer, Inc., Wellesley, MA), 2 mM mannosyl peptide (Ac-Ala-Ala-Pro-Thr-(Man)-Pro-Val-Ala-Ala-Pro-NH_2), 10 mM $MnCl_2$, 2% Triton X-100, 5 mM AMP, 200 mM GlcNAc, 10% glycerol, and 100 μg of microsomal membrane fraction was incubated at 37 °C for 1 h. After boiling for 3 min, the mixture was analyzed by reverse phase HPLC using a Wakopak 5C18-200 column (4.6 × 250 mm, Wako Pure Chemical Industries, Osaka, Japan). The gradient solvents were aqueous 0.1% trifluoroacetic acid (solvent A) and acetonitrile containing 0.1% trifluoroacetic acid (solvent B). The mobile phase consisted of 100% A for 10 min and then a linear gradient to 75% A:25% B over 25 min. Peptide separation was monitored at 214 nm, and the radioactivity of each fraction (1 ml) was measured using a liquid scintillation counter.

4.3. Antibodies

All antibodies used in Western blotting, immunohistochemistry, and FACS are listed in Supplementary Table 1.

4.4. Histology and immunohistochemical analysis

Muscle cryosections (6–10 μm) were stained with hematoxylin and eosin (H&E), or treated with 0.1% Triton X-100, blocked with 5% goat serum/1% BSA in PBS, then incubated with primary antibodies (Supplementary Table 1) at 4 °C overnight. After washing with PBS, specimens were incubated with a secondary antibody labeled with Alexa Fluor 488 or Alexa Fluor 568 (1:200–400 dilution; Molecular Probes) at RT for 1 h, counterstained with TOTO-3 (1:5000; Molecular Probes), and then mounted in Vectashield (Vector). The images were recorded using a confocal laser scanning microscope system TCSSP™ (Leica). For fiber size measurement, cross-sections of muscle were stained with anti-laminin α2

antibody and recorded and quantified by a digital microscope, BIOREVO (http://www.biorevo.jp; KEYENCE, Osaka, Japan).

4.5. Western blotting

Western blotting was performed as previously described (Hosaka et al., 2002). In brief, 20 μg of muscle proteins were separated on 7.5% SDS–PAGE gels and transferred to a PVDF membrane (Millipore, Bedford, MA). After incubation with primary antibodies (Supplementary Table 1), the membranes were incubated in HRP-labeled secondary antibodies (1:5000 dilution) (Amersham Biosciences, UK). The signals were detected by using an ECL plus Western Blotting Detection System (GE Healthcare, Buckinghamshire, UK).

4.6. Laminin blot overlay assay

An overlay assay was performed as described by Moore et al. (2002). In brief, WGA-enriched homogenates were prepared from wild-type and *POMGnT1*$^{-/-}$ brains, separated on SDS–PAGE gels, blotted onto a PDVF membrane, and incubated with mouse EHS laminin (Trevigen, Gaithersburg, MD, USA). Bound laminin was probed with anti-laminin antibody (Sigma, St. Louis, MO) and ECL system (GE Healthcare, Buckinghamshire, UK).

4.7. Single fiber preparation and culture

Single fibers were prepared from extensor digitorum longus (EDL) and soleus muscles of wild-type and *POMGnT1*$^{-/-}$ mice as described by Rosenblatt et al. (1995). Each fiber was plated onto Matrigel (BD Biosciences, Bedford, MA)-coated 24-well plates and cultured in growth medium for 3 days. Then, the number of cells around the parental fiber was counted.

4.8. Isolation of satellite cells, proliferation assay, and fusion index

Satellite cells were prepared from wild-type and *POMGnT1*$^{-/-}$ mice by FACS as previously described (Fukada et al., 2007). Sorted cells were plated on Matrigel-coated 24-well-plates at a density of 1×10^4 cells/well in a growth medium, DMEM (High glucose; Wako, Osaka), supplemented with 20% fetal bovine serum (Equitech-bio, Inc., Kerville, TX), human recombinant bFGF (2.5 ng/ml) (Invitrogen), recombinant mouse HGF (25 ng/ml) (R&D Systems, Minneapolis, MN), and heparin (5 μg/ml) (Sigma). For the MTT assay, 100 μl of 0.5% MTT (3-(4,5-dimethylthiazol-2-yl)-2,5-diphenyltetrazolium bromide) (Dojindo, Kumamoto, Japan) was added to the culture at each time point, and after 4 h incubation, the cells were collected in 1 ml of acid isopropanol solution. OD_{590} was measured and plotted. After reaching 70% confluency, the cells were induced to differentiate into myotubes by low-serum medium (5% horse serum/DMEM), and 18 h later, the cells were fixed, stained with anti-sarcomeric α-actinin antibody and DAPI (nuclei). Fusion index was calculated as (the numbers of nuclei in the myotubes/total nuclei) × 100%.

4.9. Production of retrovirus vectors

pMXs-IG (Kitamura et al., 2003) was kindly provided by T.Kitamura at Tokyo University. Human POMGnT1 cDNA, which has an Xpress epitope and a His-tag at the N-terminal (Akasaka-Manya et al., 2004), was cloned into the multi-cloning site upstream of IRES-GFP of the vector. Vector particles were produced by transfection of the vector plasmid into PLAT-E packaging cells (Kitamura et al., 2003). Proliferating satellite cells (myoblasts) were incubated with the viral vectors overnight and 4 days later, successfully transduced GFP-positive cells were collected by FACS, and the proliferation rate was evaluated by MTT assay.

4.10. Electron microscopy

Mice were perfused transcardially with a solution of 2% paraformaldehyde and 2.5% glutaraldehyde in PBS under deep pentobarbital anesthesia. The anterior tibial muscles were excised, embedded in 3% agarose, and sections (70 μm in thickness) were prepared on a Vibratome. Sections were fixed in OsO_4, ehydrated, and embedded in Cartepoxy resin. Ultrathin sections were prepared, stained with lead citrate and uranyl acetate, and observed under a Hitachi H-7000 transmission electron microscope.

4.11. Measurement of serum creatine kinase (CK)

Blood samples were obtained from the tail vein or directly from the heart at sacrifice. Serum CK level was measured by colorimetric assay using an FDC3500 clinical biochemistry autoanalyzer (FujiFilm Medical Co., Tokyo, Japan).

4.12. Cardiotoxin (CTX) injection

To induce muscle regeneration, CTX (10 μmol/L in saline; Sigma, St. Louis, MO) was injected into the tibialis anterior (TA) muscles three times at indicated intervals. The muscle cross-sections were stained with Oil red O (Muto Pure Chemicals Co., Ltd., Tokyo, Japan) to detect lipid droplets, or with Sirius red F3B (Sigma Chemical Co., St. Louis, MO) in saturated picric acid to stain collagen fibers.

Acknowledgments

This work was supported by Health Science Research Grants for Research on the Human Genome and Gene Therapy (H16-genome-003). For research on Phychiatric and Neurological Diseases and Mental Health (H18-kokoro-019; H20-016) from the Japanese Ministry of Health, Labor and Welfare, and Grants-in-Aid for Scientific Research (18590392) from the Japanese Ministry of Education, Culture, Sports, Science and Technology.

Appendix A. Supplementary data

Supplementary data associated with this article can be found, in the online version, at doi:10.1016/j.mod.2008.12.001.

REFERENCES

Akasaka-Manya, K., Manya, H., Kobayashi, K., Toda, T., Endo, T., 2004. Structure–function analysis of human protein O-linked mannose beta1,2-N-acetylglucosaminyltransferase 1, POMGnT1. Biochem. Biophys. Res. Commun. 320, 39–44.

Blau, H.M., Webster, C., Pavlath, G.K., 1983. Defective myoblasts identified in Duchenne muscular dystrophy. Proc. Natl. Acad. Sci. USA 80, 4856–4860.

Burkin, D.J., Wallace, G.Q., Milner, D.J., Chaney, E.J., Mulligan, J.A., Kaufman, S.J., 2005. Transgenic expression of α7β1 integrin maintains muscle integrity, increases regenerative capacity, promotes hypertrophy, and reduces cardiomyopathy in dystrophic mice. Am. J. Pathol. 166, 253–263.

Burkin, D.J., Wallace, G.Q., Nicol, K.J., Kaufman, D.J., Kaufman, S.J., 2001. Enhanced expression of the alpha 7 beta 1 integrin reduces muscular dystrophy and restores viability in dystrophic mice. J. Cell Biol. 152, 1207–1218.

Campanelli, J.T., Roberds, S.L., Campbell, K.P., Scheller, R.H., 1994. A role for dystrophin-associated glycoproteins and utrophin in agrin-induced AChR clustering. Cell 77, 663–674.

Cohn, R.D., Henry, M.D., Michele, D.E., Barresi, R., Saito, F., Moore, S.A., Flanagan, J.D., Skwarchuk, M.W., Robbins, M.E., Mendell, J.R., Williamson, R.A., Campbell, K.P., 2002. Disruption of DAG1 in differentiated skeletal muscle reveals a role for dystroglycan in muscle regeneration. Cell 110, 639–648.

Endo, T., Toda, T., 2003. Glycosylation in congenital muscular dystrophies. Biol. Pharm. Bull. 26, 1641–1647.

Fukada, S., Uezumi, A., Ikemoto, M., Masuda, S., Segawa, M., Tanimura, N., Yamamoto, H., Miyagoe-Suzuki, Y., Takeda, S., 2007. Molecular signature of quiescent satellite cells in adult skeletal muscle. Stem Cells 25, 2448–2459.

Gee, S.H., Montanaro, F., Lindenbaum, M.H., Carbonetto, S., 1994. Dystroglycan-alpha, a dystrophin-associated glycoprotein, is a functional agrin receptor. Cell 77, 675–686.

Hosaka, Y., Yokota, T., Miyagoe-Suzuki, Y., Yuasa, K., Imamura, M., Matsuda, R., Ikemoto, T., Kameya, S., Takeda, S., 2002. Alpha1-syntrophin-deficient skeletal muscle exhibits hypertrophy and aberrant formation of neuromuscular junctions during regeneration. J. Cell Biol. 158, 1097–1107.

Hu, H., Yang, Y., Eade, A., Xiong, Y., Qi, Y., 2007. Breaches of the pial basement membrane and disappearance of the glia limitans during development underlie the cortical lamination defect in the mouse model of muscle–eye–brain disease. J. Comp. Neurol. 502, 168–183.

Ibraghimov-Beskrovnaya, O., Ervasti, J.M., Leveille, C.J., Slaughter, C.A., Sernett, S.W., Campbell, K.P., 1992. Primary structure of dystrophin-associated glycoproteins linking dystrophin to the extracellular matrix. Nature 355, 696–702.

Kanagawa, M., Michele, D.E., Satz, J.S., Barresi, R., Kusano, H., Sasaki, T., Timpl, R., Henry, M.D., Campbell, K.P., 2005. Disruption of perlecan binding and matrix assembly by post-translational or genetic disruption of dystroglycan function. FEBS Lett. 579, 4792–4796.

Kanagawa, M., Toda, T., 2006. The genetic and molecular basis of muscular dystrophy: roles of cell-matrix linkage in the pathogenesis. J. Hum. Genet. 51, 915–926.

Kitamura, T., Koshino, Y., Shibata, F., Oki, T., Nakajima, H., Nosaka, T., Kumagai, H., 2003. Retrovirus-mediated gene transfer and expression cloning: powerful tools in functional genomics. Exp. Hematol. 31, 1007–1014.

Liu, J., Ball, S.L., Yang, Y., Mei, P., Zhang, L., Shi, H., Kaminski, H.J., Lemmon, V.P., Hu, H., 2006. A genetic model for muscle–eye–brain disease in mice lacking protein O-mannose 1,2-N-acetylglucosaminyltransferase (POMGnT1). Mech. Dev. 123, 228–240.

Liu, J., Burkin, D.J., Kaufman, S.J., 2008. Increasing alpha 7 beta 1-integrin promotes muscle cell proliferation, adhesion, and resistance to apoptosis without changing gene expression. Am. J. Physiol. Cell Physiol. 294, C627–C640.

Michele, D.E., Barresi, R., Kanagawa, M., Saito, F., Cohn, R.D., Satz, J.S., Dollar, J., Nishino, I., Kelley, R.I., Somer, H., Straub, V., Mathews, K.D., Moore, S.A., Campbell, K.P., 2002. Post-translational disruption of dystroglycan–ligand interactions in congenital muscular dystrophies. Nature 418, 417–422.

Moore, S.A., Saito, F., Chen, J., Michele, D.E., Henry, M.D., Messing, A., Cohn, R.D., Ross-Barta, S.E., Westra, S., Williamson, R.A., Hoshi, T., Campbell, K.P., 2002. Deletion of brain dystroglycan recapitulates aspects of congenital muscular dystrophy. Nature 418, 422–425.

Peng, H.B., Ali, A.A., Daggett, D.F., Rauvala, H., Hassell, J.R., Smalheiser, N.R., 1998. The relationship between perlecan and dystroglycan and its implication in the formation of the neuromuscular junction. Cell Adhes. Commun. 5, 475–89.

Rosenblatt, J.D., Lunt, A.I., Parry, D.J., Partridge, T.A., 1995. Culturing satellite cells from living single muscle fiber explants. In Vitro Cell Dev. Biol. Anim. 31, 773–779.

Sandri M., 2008. Signaling in muscle atrophy and hypertrophy. Physiology (Bethesda) 23, 160–170.

Sugita, S., Saito, F., Tang, J., Satz, J., Campbell, K., Südhof, T.C., 2001. A stoichiometric complex of neurexins and dystroglycan in brain. J. Cell Biol. 154, 435–445.

Voit, T., Tome, F.S., 2004. The congenital muscular dystrophies. In: Engel, A.G., Franzini-Armstrong, C. (Eds.), Myology. McGraw-Hill, New York, pp. 1203–1238.

Yang, Y., Zhang, P., Xiong, Y., Li, X., Qi, Y., Hu, H., 2007. Ectopia of meningeal fibroblasts and reactive gliosis in the cerebral cortex of the mouse model of muscle–eye–brain disease. J. Comp. Neurol. 505, 459–477.

Yoshida, A., Kobayashi, K., Manya, H., Taniguchi, K., Kano, H., Mizuno, M., Inazu, T., Mitsuhashi, H., Takahashi, S., Takeuchi, M., Herrmann, R., Straub, V., Talim, B., Voit, T., Topaloglu, H., Toda, T., Endo, T., 2001. Muscular dystrophy and neuronal migration disorder caused by mutations in a glycosyltransferase, POMGnT1. Dev. Cell 1, 717–724.

A Renaissance for Antisense Oligonucleotide Drugs in Neurology

Exon Skipping Breaks New Ground

Toshifumi Yokota, PhD; Shin'ichi Takeda, MD, PhD; Qi-Long Lu, MD, PhD; Terence A. Partridge, PhD; Akinori Nakamura, MD, PhD; Eric P. Hoffman, PhD

Antisense oligonucleotides are short nucleic acid sequences designed for use as small-molecule drugs. They recognize and bind to specific messenger RNA (mRNA) or pre-mRNA sequences to create small double-stranded regions of the target mRNA that alter mRNA splicing patterns or inhibit protein translation. Antisense approaches have been actively pursued as a form of molecular medicine for more than 20 years, but only one has been translated to a marketed drug (intraocular human immunodeficiency virus treatment). Two recent advances foreshadow a change in clinical applications of antisense strategies. First is the development of synthetic DNA analogues that show outstanding stability and sequence specificity yet little or no binding to modulator proteins. Second is the publication of impressive preclinical and clinical data using antisense in an exon-skipping strategy to increase dystrophin production in Duchenne muscular dystrophy. As long-standing barriers are successfully circumvented, attention turns toward scale-up of production, long-term toxicity studies, and the challenges to traditional drug regulatory attitudes presented by tightly targeted sequence-specific drugs.

Arch Neurol. 2009;66(1):32-38

With the advent of recombinant DNA in the 1970s, it was soon realized that bacteria possess a form of regulatory machinery where small RNA transcripts can bind (hybridize) to other target RNAs and inhibit the translation of these targets.[1] These antisense RNAs were subsequently recognized as natural translational regulation mechanisms in plants and higher organisms.[2] More recently, a specialized form of antisense transcript was found to be a cellular defense mechanism against invading messenger RNAs (mRNAs) (viruses), and this has been harnessed as a popular method to "knock down" specific mRNA transcripts in cultured cell models (short interfering RNAs).[3]

Attention soon shifted toward development of antisense molecules as a form of small-molecule drug (antisense oligonucleotide [AO]). The approach was intuitive: one needs simply to chemically synthesize short pieces of DNA of about 20 bases, where a specific complementary sequence is designed to hybridize with a desired target mRNA. Such designer AO drugs should show very high specificity and selectivity for binding only the desired target RNA sequence of nucleotides that is predicted by base pairing. Beginning in the mid-1980s, this approach was put to the test in model systems and was shown to work quite well in shutting down the production of the target (undesired) protein.[4] Isis Pharmaceuticals, Inc, Carlsbad, California, a company focused on clinical applications of AOs, was incorporated in 1989. Additional companies focusing on AO approaches soon followed.

Despite early promise, uses of AOs as small-molecule drugs have been painfully slow to enter the market and standard of care. Indeed, only a single AO drug has been approved by the Food and Drug

Author Affiliations: Research Center for Genetic Medicine, Children's National Medical Center, Washington, DC (Drs Yokota, Partridge, and Hoffman); Department of Molecular Medicine, National Institutes for Neuroscience, Tokyo, Japan (Drs Takeda and Nakamura); and McColl-Lockwood Laboratory for Muscular Dystrophy Research, Neuromuscular/ALS Center, Carolinas Medical Center, Charlotte, North Carolina (Dr Lu).